FORSCHUNGSZENTRUM JÜLICH GmbH

Zentralabteilung für Chemische Analysen

Neutron Activation Analysis: Techniques and Relevant Nuclear Data

Gerhard Erdtmann

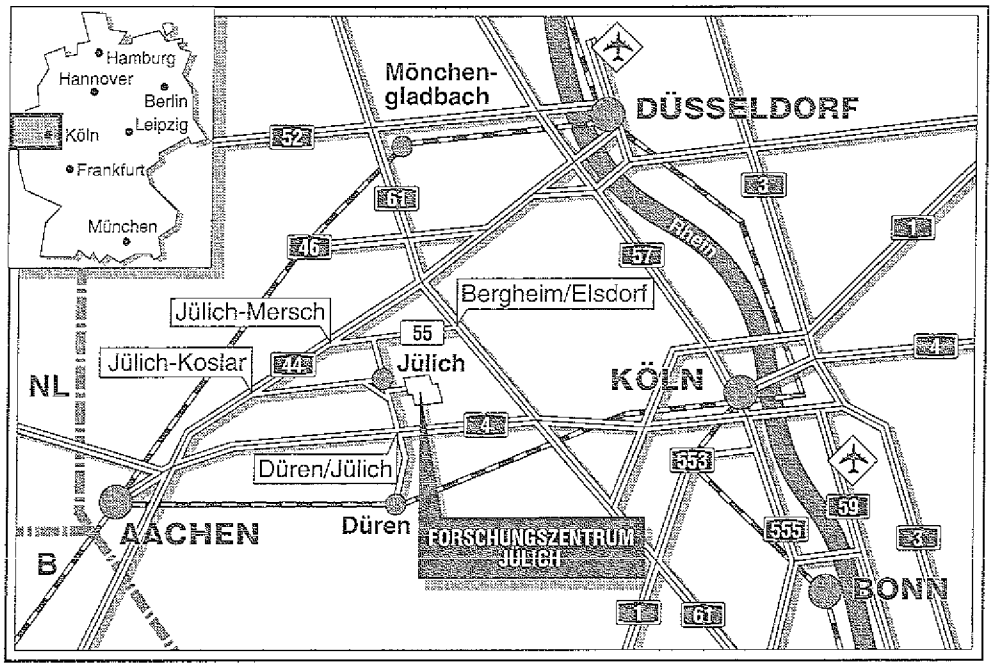

Berichte des Forschungszentrums Jülich ; 2673
ISSN 0366-0885
Zentralabteilung für Chemische Analysen Jül-2673

Zu beziehen durch: Forschungszentrum Jülich GmbH · Zentralbibliothek
Postfach 1913 · D-5170 Jülich · Bundesrepublik Deutschland
Telefon: 02461/61-6102 · Telefax: 02461/61-6103 · Telex: 833556-70 kfa d

Neutron Activation Analysis: Techniques and Relevant Nuclear Data

Gerhard Erdtmann

Revised and extended manuscript of a lecture held at the *"International Atomic Energy Agency Advanced Interregional Training Course on Sampling, Sample Preparation and Data Evaluation for Trace Analysis of Elements and Radionuclides by Nuclear and Instrumental Methods"* at the Research Center Jülich, Nov. 6 to Dec. 2, 1989.

NEUTRONENAKTIVIERUNGSANALYSE: VERFAHREN UND NUKLEARE DATEN

Kurzfassung

Der Bericht entstand aus einer Vorlesung im Rahmen eines IAEA Fortbildungskurses über Spurenelementanalytik und aus den Einführungen zu praktischen Übungen in unserem Laboratorium. Im ersten Teil (Abschnitte 1 bis 4) wird, anhand einer statistischen Übersicht über die Anwendungen der verschiedenen Methoden der Aktivierungsanalyse und die bisherigen Entwicklungstendenzen, die praktische Bedeutung der Reaktorneutronenaktivierungsanalyse (RNAA) dargestellt, und die Techniken - Bestrahlungseinrichtungen und γ-Spektrometrie - werden kurz beschrieben. Der zweite Teil (Abschnitte 5 und 6) befaßt sich mit den Standardisierungsmethoden der RNAA - Absolutmethode, Relativmethode, Monostandard- einschließlich k_0-Methode. Das in der Abteilung Radioanalytik der ZCH/KFA verwendete Verfahren wird eingehender behandelt. Eine vollständige Tabelle der dafür benötigten nuklearen Daten (Halbwertzeiten, k_i – , Q_0- und $\bar{E}_r$-Werte) ist in diesem Abschnitt enthalten. Zum Schluß werden potentielle Fehlerquellen betrachtet und die Fehlerfortpflanzung auf das Analysenergebnis dargestellt.

NEUTRON ACTIVATION ANALYSIS: TECHNIQUES AND RELEVANT NUCLEAR DATA

Summary

The report is based on a lecture held at an IAEA training course on trace element analysis and on the introductions given for some practical exercises in our laboratory during this course. In its first part (Chapters 1 to 4) from a statistical review on the applications of the different methods of activation analysis the practical importance of neutron activation analysis (NAA) and expecially of reactor NAA is made obvious. The techniques - irradiation facilities and γ-spectrometry - are basically described. In the second part (Chapters 5 and 6) the different standardization techniques - absolute method, relative method and single monitor including the k_0-method - are presented. The procedure used in the Radioanalytical Section of the ZCH/KFA, which is based on the k_0 method - is thoroughly treated. In this section a Table of all nuclear parameters which are required for the calculation of amounts of elements is included. Sources of error are treated including those of the nuclear data. The propagation of the different types of error to the analytical results is discussed in detail.

Contents

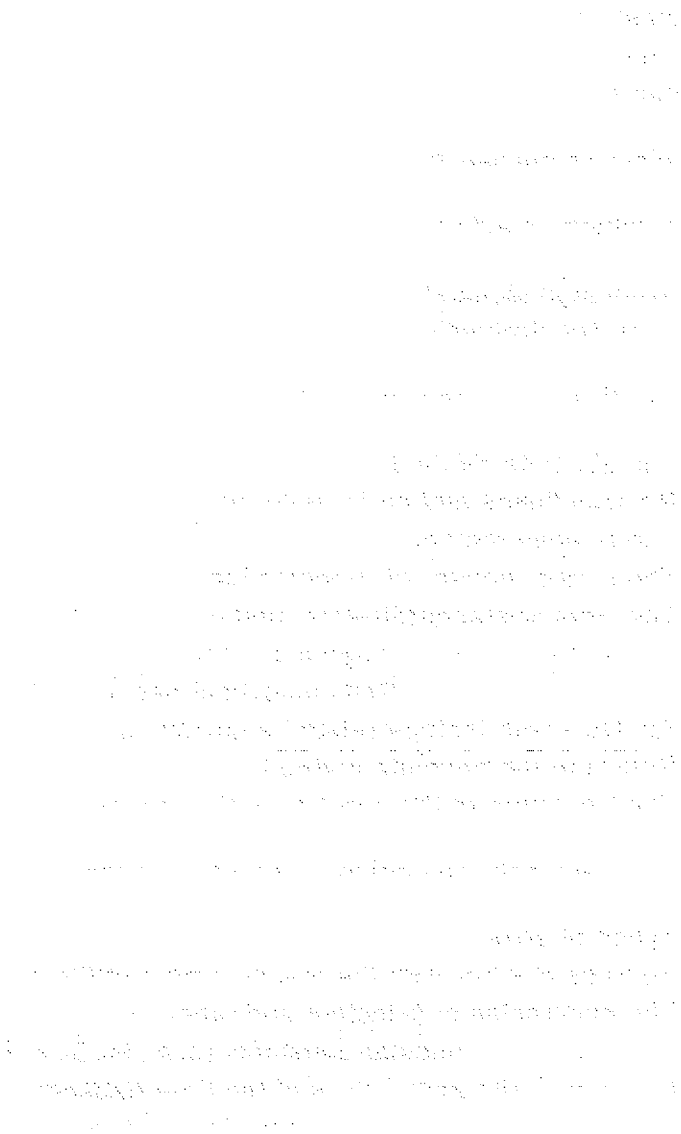

1. The place of nuclear techniques in analytical chemistry

Since the discovery of radioactivity, radionuclides and nuclear methods have been applied in analytical chemistry. A prerequisite for these applications was the knowledge of the properties of radionuclides - half-lives, decay modes and energies, cross-sections - and their quantitative determination. With the measurement of these nuclear data methods of chemical analysis - mainly separation and quantification techniques - were widely used. These numerous interactions between analytical and nuclear chemistry still continue and are treated by the scientific discipline of nuclear or radioanalytical chemistry. It provides a great number of different methods and techniques which are listed in Table 1.

If one accepts the number of publications to be a measure of the importance of an analytical method, then that of nuclear methods can be estimated from an investigation of BRAUN [1] (Fig.1). He reviewed about 7000 papers in analytical chemistry published between 1981 and 1984, and found, that more than 60% deal with optical methods. There is no question, that methods such as atomic absorption spectrometry, spectrophotometry and emission spectrometry are the working horses in elemental analysis. But already the next group is nuclear methods, and out of these just the activation methods are even more often used than X-ray, chromatographic, or electrochemical methods.

In Fig. 2 is shown, where and for what purposes activation analysis is used. These plots are based on a literature search of GUINN [2] made on papers published in the Americas from 1976 to 1983. About one half of the papers is published by universities, one quarter by federal and state laboratories, and the rest comes from medical and industrial laboratories. Three quarters report on applications and one quarter on the development of methods and techniques. The largest part of the applications is with the industry. We may assume, that this part is even larger because many industrial applications are not described in public journals. The rest is nearly equally distributed between applications in medicine, environmental and agricultural sciences and, finally, the sciences dealing with the mineral composition of earth and extraterrestrial matter, geo- and cosmochemistry.

Activation analysis is based on nuclear reactions where radioactive nuclides are produced from stable, natural nuclides. The nuclear reactions can be induced by protons or other light nuclei, by photons or by neutrons. Fig. 3 shows the shares of these activation techniques on the total amount on papers in activation analysis. The results found by GUINN [2] for the period 1976 - 1983 are compared with those from an evaluation of papers published until 1971, based on the bibliography of LUTZ et al.[3] One sees on the top that neutrons are the predominantly used activation particles and that their share has even increased from the early periods of activation analysis ($\simeq$1950 - 1971) to the more recent period 1976 - 1983. Neutrons can be obtained from different types of sources and reactors are most often used for activation analysis. From the diagrams in the middle it is seen, that their use has increased, whereas that of neutron generators was on the decline. In the diagrams below, finally, there is shown, that out of the neutron spectrum of a reactor the thermal neutrons are of predominant importance for activation analysis.

Table 1 - Nuclear Methods of Chemical Analysis

- **Activation analysis methods**, e.g.
  - *Reactor neutron activation analysis*
    - thermal neutron activation analysis
    - epithermal neutron activation analysis
    - fast reactor neutron activation analysis
      These three methods can be carried out as
      - *instrumental neutron activation analysis*
      - *radiochemical neutron activation analysis*
    - prompt γ-neutron activation analysis
    - neutron depth profiling
  - ***14-MeV neutron activation analysis with neutron generators***
  - ***Neutron activation analysis with isotope neutron sources***
  - ***Charged particle activation analysis***
    - activation analysis with protons
    - activation analysis with deuterons
    - activation analysis with He-3 particles
    - activation analysis with H-3 particles
    - activation analysis with He-4 particles
  - ***Photon activation analysis***
- **Tracer techniques**
- **Isotope dilution analysis**
- **Radionuclide excited X-ray fluorescence analysis**
- **Radiochemical and radiometric techniques**
  for the determination of radioactive components of matter
- **Autoradiographic techniques**

The upper circle of Fig. 4 shows, that 44% of the work was done with low flux reactors, such as those of the SLOWPOKE or TRIGA type, and 56% have used medium and high flux reactors with fluxes $> 10^{13}$ n cm^{-2} s^{-1}. From the lower circle it can be seen, that more than 50% of the analyses are carried out by instrumental techniques and the other half is distributed between radiochemical neutron activation analysis (RCS-NAA), prompt γ-neutron activation analysis (PG-NAA), activation analysis with chemical separations before the irraditaion (pre-irradiation separation NAA, PIS-NAA) and a variety of further techniques.

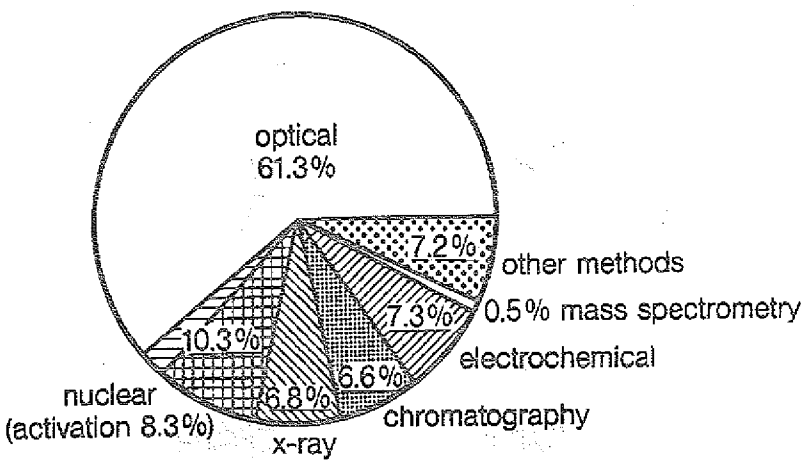

Figure 1 - Use of instrumental techniques in chemical analysis *(after data of BRAUN [1], having reviewed 6852 papers published between 1981 and 1984).*

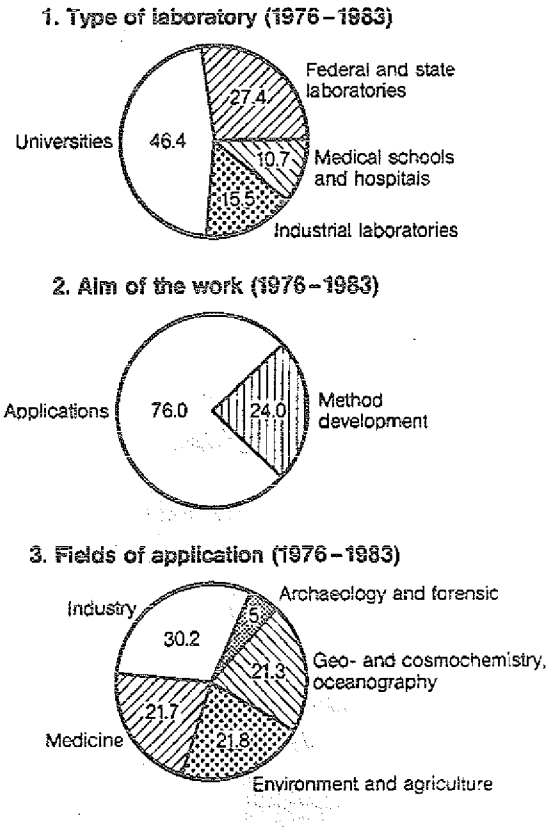

Figure 2 - Statistical reviews on papers in activation analysis considering the type of laboratory, where the work was carried out, the aim of the work and the fields of application *(after data of GUINN [2], having reviewed 243 papers published in the Americas between 1976 and 1983).*

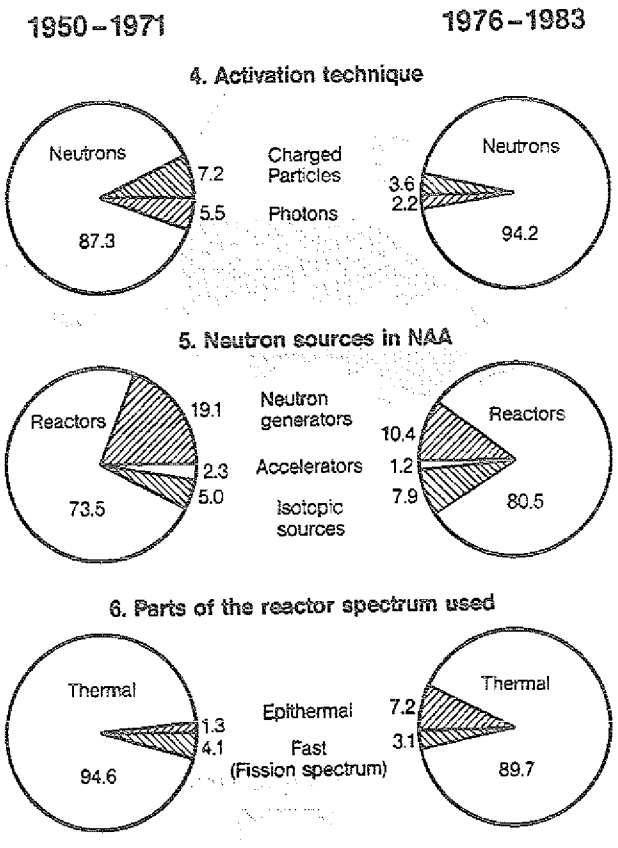

Figure 3 - Statistical reviews on papers in activation analysis considering the activation techniques, the neutron sources and the type of neutrons used. *(based on an evaluation of the bibliography of LUTZ et al.[3] for papers until 1971 and on data of GUINN [2], see Fig. 2).*

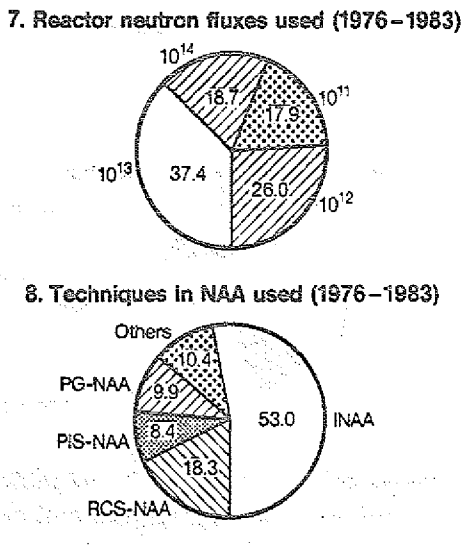

Figure 4 - Statistical reviews on papers in reactor neutron activation analysis considering the fluxes and the techniques used *(source of data see Fig. 2).*

From this introduction and the figures the following should be learned:

1. It is not correct to talk about "*the* activation analysis method", as it is often heard. We have seen, that there are at least about 20 different methods using quite different techniques and instruments, which can be subsumed under activation analysis.

2. Reactor neutron activation analysis comprehends the most widely used group of methods and this predominance is so large, that in colloquial language activation analysis is usually understood as reactor neutron activation analysis.

In our group, the Radiochemical Analysis Section of the Central Division of Chemical Analysis (ZCH) of the Research Center Jülich (KFA), also more than 90% of activation analyses are carried out using the reactor and instrumental techniques. Therefore, and because practical exercises during this course will deal with these techniques, the following explications shall be restricted to reactor neutron activation analysis, and the short forms NAA or activation analysis mean this group of methods.

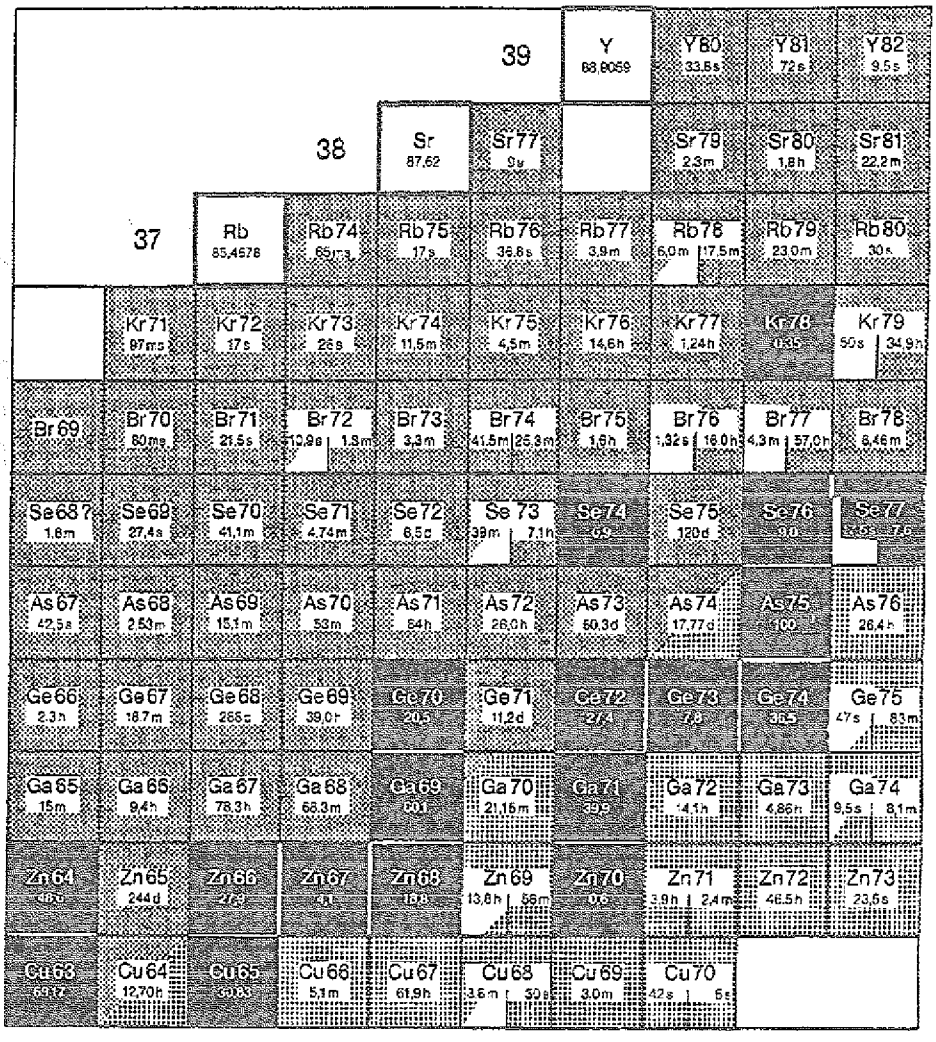

Figure 5 - Section of a nuclide chart [4]

2. The principle of activation analysis

Activation analysis is based on reactions of atomic nuclei. The nuclides or isotopes of the elements are systematically arranged in a "Chart of the Nuclides" [4], of which a section is shown in a simplified depiction in Fig. 5. All nuclides in a horizontal row belong to the same element. The stable isotopes are marked by black squares. They are the constituents of our world, of all matter surrounding us. The nuclides at the left side of the stable ones are instable because they have an excess of protons. They decay by the emission of β^+-radiation or by the capture of electrons from the inner atomic shells. The nuclides at the right side of the stable ones are instable because they have an excess of neutrons. They decay by the emission of β^--radiation. Independent of the type of β-decay the particle emission is, with most nuclides, accompanied by the emission of photons, the γ-radiation, which is most useful for the iden-

tification of unknown radionuclides. If atoms of stable elements are exposed to a flux of neutrons, then they may capture them and produce new, usually radioactive, atoms. In most cases (n,γ)-reactions take place, i.e. the new nuclides are generated in an excited, high-energy state, which is de-excited by the emission of γ-rays.

It should be mentioned here, that this "prompt" γ-radiation must not be confused with the "delayed" γ-radiation emitted by radionuclides, which is usually measured in instrumental activation analysis, whereas the "prompt" radiation is measured if "prompt activation analysis" is carried out, which is not within the scope of this lecture.

With a (n,γ)-reaction on a stable nuclide always the nuclide at the right side is produced. Many of these new nuclides are instable and can be identified by their radioactivity.

2a. Irradiation facilities

The most intensive neutron sources are the nuclear reactors, and this is one of the reasons, why reactor neutron activation analysis is the most often used technique, as has been outlined in the previous section. Many research reactors are of the so called swimming pool type (Fig. 6). The reactor core, where the neutrons are generated, is situated at the bottom of the water tank which serves for three purposes:

- Moderation of neutrons,
- cooling of the core,
- shielding from the intensive radiation of the core.

To irradiate a sample, it has to be placed near the core. A simple, hand driven facility is shown in Fig. 6.

The sample container is hung on a hook of a rope and it is sinked to the core by means of a winch. A tube, fitted to the place of a fuel element, leads and keeps the capsule in its place. When the irradiation time is over, the sample is lifted by the winch to an opening in the tube, through which the sample can be taken using the grab pole. The opening is under water, which shields the operator from the radiation of the sample. The sample is moved to a lead container, which is drawn out of the water pool when the dose rate at its surface is low enough.

A more common type of irradiation facilities are rabbit tube systems, which allow faster transport of the samples.

At our research center, there is a tank type reactor, FRJ-2 (DIDO). The water tank is closed and irradiation facilities have to be placed in one of the beam tubes. Such a facility, carried out as a revolver magazine, is shown in Fig. 7.

It is installed in a beam tube ending in the graphite reflector of the reactor. At the left side is the reactor core, where the neutrons are generated. Then a section of the tank is seen, containing heavy water (D_2O) which acts as a neutron moderator. The graphite layer outside the tank serves to moderate and to reflect neutrons. The lead and the

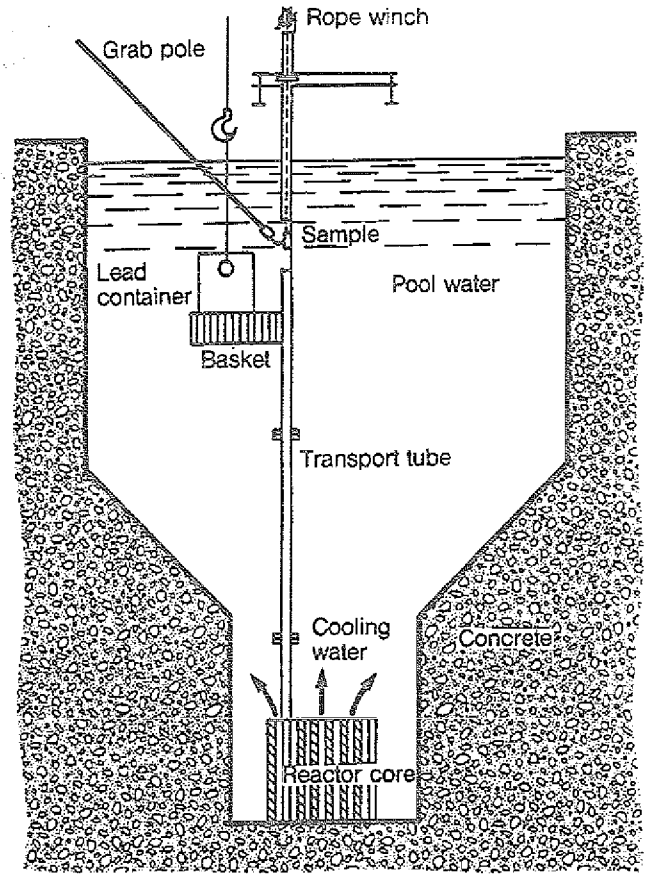

Figure 6 - "In-core insertion tube" irradiation facility in a swimming pool reactor.

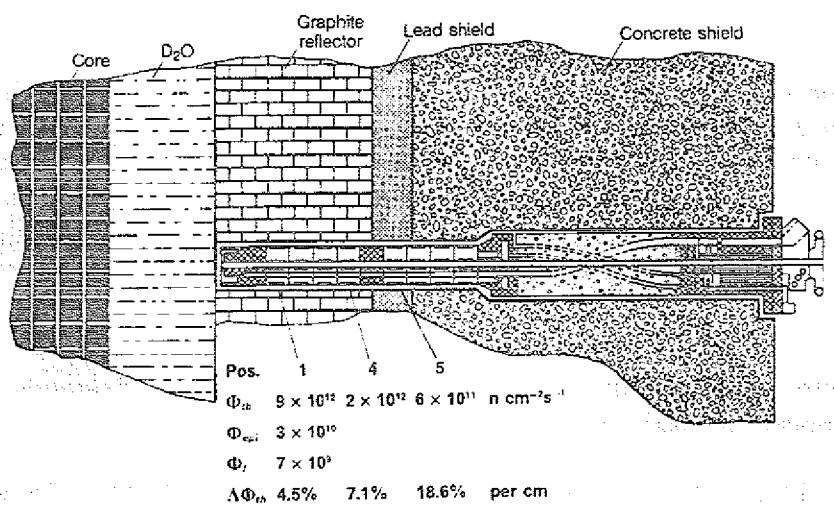

Figure 7 - Beam tube irradiation facility (revolver magazine, Hobson unit) in the FRJ-2, KFA Jülich *(from Ref.[5])*

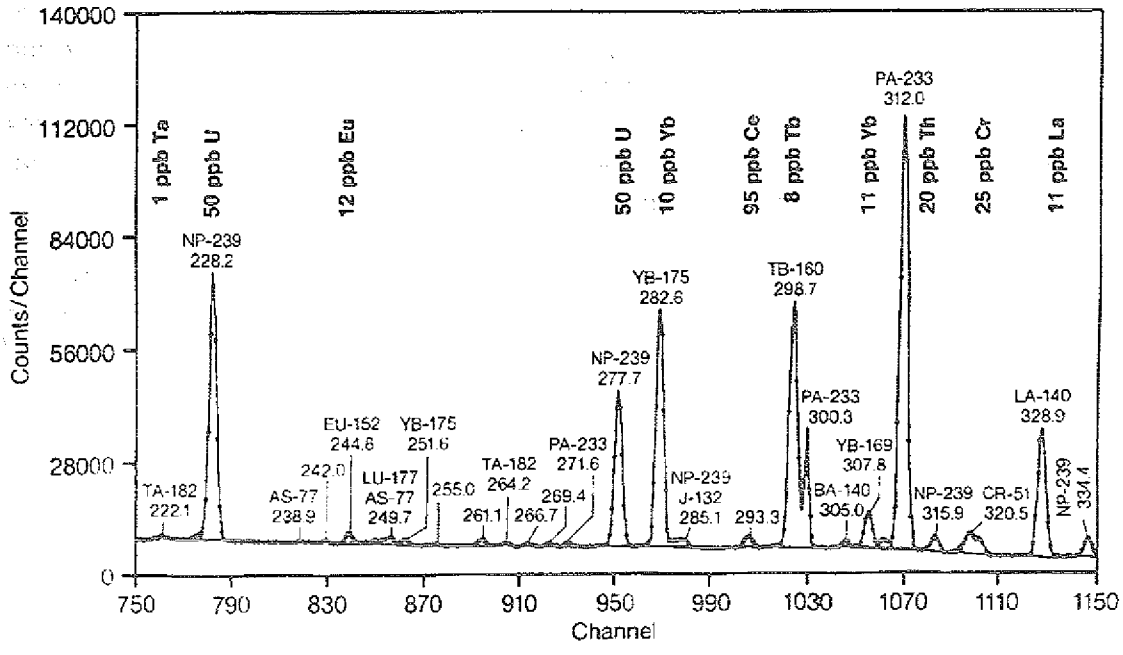

Figure 8 - Section of a γ-ray spectrum.

concrete shields absorb the γ- radiation emitted from the core and a cadmium liner near the lead shield (not shown in the figure) absorbs neutrons.

The facility contains eight magazines, each with seven positions, which can be filled with samples to be irradiated. The approximate neutron fluxes in three of the magazines are indicated.

With magazines 1, 4 and 5 the approximate mean fluxes are indicated. (Φ_{th}, Φ_{epi}, Φ_f = thermal, epithermal and fast flux, $\Delta\Phi_{th}$ = horizontal thermal flux gradient).

2b. γ-ray spectrometry

When a sample has been irradiated, it contains many radioactive atoms of different species according to the chemical elements the sample is composed of. These radionuclides can be identified by their half-life and by the β- and the γ-radiation they emit. The most convenient and effective way is the measurement of the γ-ray spectrum. A section of such a spectrum is shown in Fig. 8. A number of discrete lines or peaks can be seen which are indicative for the radionuclides. They are situated on a "background continuum", which is caused by Compton scattering and backscattering of the γ-radiation and by bremsstrahlung from the β-radiation emitted by the sample. It is usually an interfering feature of the γ-spectrum, limiting the sensitivity of the analytical procedure.

The situation of a peak along the x-axis marks its energy, which is characteristic for a certain nuclide. The height of the peak, or better its area, is a measure for the activity of the corresponding nuclide, i.e. it indicates, how many atoms of this type of

nuclide have been produced. γ-ray spectra are usually evaluated by computer programs which find the lines, determine their energies and the peak areas. With additional computer programs and nuclide libraries also the radionuclides can be identified and their decay rates calculated. The spectrum shown has already been evaluated and the γ-ray energies and the corresponding radionuclides are indicated at the tops of the lines. The automatic evaluation of series of γ-spectra including the calibration of the γ-ray spectrometer (or, more precise, the calibration of a certain counting position or arrangement with respect to the peak counting efficiencies), is treated in more detail in the practical exercises of this course. Here we just want to keep in mind, that we can determine ***peak areas***, which are the numbers of counts in the peaks, ***peak counting rates***, which are the numbers of counts in a peak per second, and ***decay rates*** or ***activities***, which are the numbers of decay events per second (Becquerel, Bq) of the radionuclides, from which the peaks are generated.

3. Standardization techniques of INAA and calculation of results

From the peak areas, the count rates or the decay rates the amounts of elements in a sample have to be calculated. Several methods can be used for this purpose and they shall be treated under the names

- Absolute method
- Relative method
- Single monitor or monostandard method
- Gent k_0-method.

3a. The absolute method

The calculation of results by this technique is based on the ***activation equation***

$$A_{0,x} = \frac{m_x\, a_x\, N_A}{M_x}\,(1 - e^{-\lambda_x t_i}) \int_{E=0}^{\infty} \sigma_x(E)\,\phi(E)dE \qquad (1)$$

where $A_{0,x}$ is the activity of the radionuclide produced from element x at irradiation end (i.e. the waiting time after irradiation is 0); m_x is the amount of element x present in the sample; a_x is the abundance of the isotope being transformed into the radionuclide found; N_A is Avogadro's number; M_x is the atomic weight; λ_x is the decay constant of the radionuclide ($\lambda_x = \ln 2/t_{1/2,x}$ with $t_{1/2,x}$ = half-life); t_i is the irradiation time; $\sigma_x(E)$ is the reaction cross section and $\phi(E)$ is the neutron flux, both depending on the neutron energy, E.

To obtain the amount of an element, m_x, present in a sample, one has to determine the experimental parameters (activity, irradiation time and neutron flux) and one has to know all the other parameters - which are natural or basic constants. The ***decay corrected absolute activity***, $A_{0,x}$, is calculated from the peak area, P_x, by

$$A_{0,x} = \frac{P_x}{\eta_x\, h_x}\;\frac{\lambda_x\, e^{\lambda_x t_w}}{1 - e^{-\lambda_x t_m}} \qquad (2)$$

with η_x = counting efficiency, h_x = γ-ray abundance, t_w = waiting time after the irradiation (required for transport and treatment of the sample, sometimes also to wait for the decay of undesired short-lived isotopes) and t_m = counting time.

The ***time parameters***, t_i, t_w and t_m can be measured. The ***counting efficiency*** is determined with samples, which have been measured by an absolute counting technique like 4π-counting, β-γ-counting, or liquid scintillation counting. Such samples are usually acquired from qualified laboratories (e.g. IAEA, Wien, or PTB, Braunschweig) in the form of calibrated solutions or solid sources. ***Avogadro's number*** is, surely, a constant and the same holds, as the name says, for the ***decay constants*** of the nuclides. ***Atomic weights*** and ***isotopic abundances*** are generally accepted as analytical constants although we know, that slight variations in the isotopic composition of some natural elements will occur. Numerical values for all these constants are readily accessible.

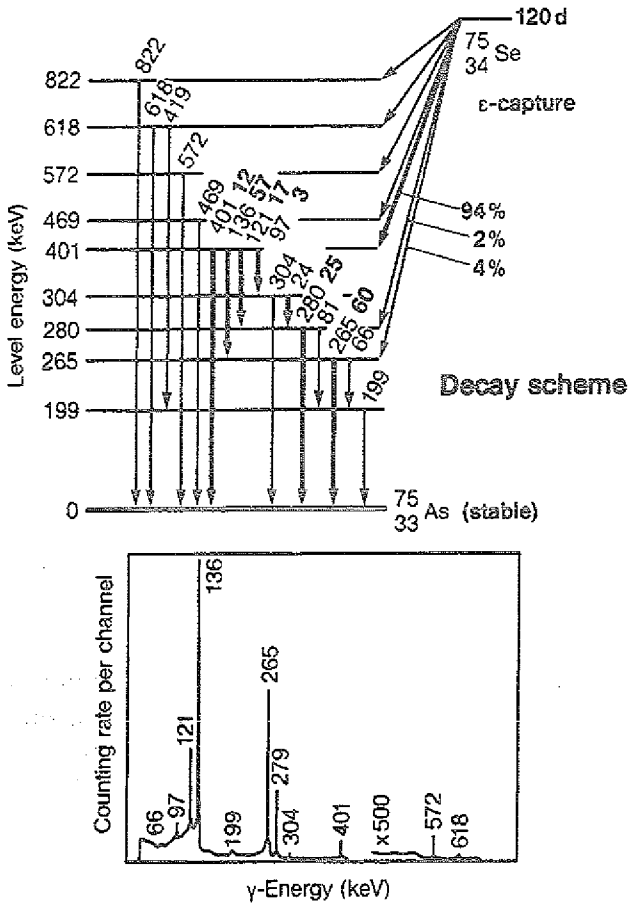

Figure 9 - Decay scheme of a radionuclide (^{75}Se) and the corresponding γ-spectrum.

The ***γ-ray abundance***, h_x, shall be explained from the decay scheme of a radionuclide (Fig. 9).

^{75}Se is chosen as an example. It has a half-life of 120 d and decays by capture of electrons from the inner atomic shells. By the decay a new nuclide, ^{75}As, With many of the decay events the new nucleus is not formed in its ground state, but in some excited state, which de-excites to the ground state by the emission of energy in the form of photons or γ-quanta. Every nuclide has many different excitation states or energy levels according to the possible modes of vibrations and rotations of its protons and neutrons and the decay process can lead to any of these levels. It is a question of chance, which of the levels is populated, but this chance is superimposed by the rules of quantum physics. The energy levels of nuclei like those of atomic electron shells, can be described by quantum numbers and spins, and between levels with special combinations of quantum numbers and spins the transitions may be allowed or more or less strongly forbidden. As a result, it is observed that certain levels have a better chance to be populated than the others. With the decay of ^{75}Se, the level of ^{75}As at 401 keV is strongly preferred and receives 94% of all decays. But also from this level only a part of the transitions decay immediately to the ground level by the emission of 401-keV γ-quanta. All other transitions lead to other intermediate levels and reach the ground

state only stepwise. In each single decay event it is a matter of chance which decay path is used, but when a large number of decays is observed one finds that each of the paths has its own, fixed probability, and accordingly each γ-transition has its own probability to occur. These transition probabilities, in percent, are indicated at the tops of the arrows. They often are identical with the γ-ray abundances. However, in some cases the γ-quantum is not emitted but its energy is transferred to a shell electron, which is then emitted. This process is called inner conversion. The transition probability is the sum of the emission probabilities or abundances of the γ-rays and the conversion electrons. The γ-ray abundances are measured for all radionuclides important with activation analysis and can be found in published tables, e.g. Ref.[6]

In the lower part of Fig. 9 the γ-spectrum of ^{75}Se is shown. The most prominent peak is that of the 136-keV γ-line, which has an abundance of 57%. The height of the 265-keV line is smaller, although the abundance of the corresponding γ-transition is nearly the same (60%). This is a consequence of the different counting efficiencies for the γ-lines. The counting efficiency of a γ-ray detector is energy dependent and for γ-energies above $\simeq$120 keV the peak counting efficiency decreases with increasing γ-energy. Many of the transitions shown in the decay scheme can not or scarcely be seen as lines in the spectrum. These weak lines are not used with the calculations of analytical results.

Now we have seen, how to measure or to find the parameters required for the numerical solution of Equation (1), except the integral term, which shall be discussed in the next Section.

3b. Neutron fluxes and cross sections

Activation analysis is mainly based on (n,γ)-reactions, which are initiated by low energy neutrons. In the neutron spectrum of a nuclear reactor (Fig. 10, lower part) they are represented by the ***thermal*** and the intermediate components. In cases, where the fast neutrons have not to be considered, the intermediate neutrons are often called ***epithermal neutrons***, as it will be done here. Neutron spectra of different reactors have always shapes similar to that shown in Fig. 10, but the ratios between the thermal, the epithermal and the fast neutrons are different and vary even inside a reactor. In the upper part of Fig. 10, the energy dependence of an activation cross section (example gold) is shown and, with respect to their complex shapes, it seems impossible, to calculate the integral of the product by folding the two curves. However, WESTCOTT [7] and HØGDAHL [8] have defined conventions for the thermal and the epithermal flux and the corresponding activation cross sections. Following HØGDAHL and omitting the subscript x we can write

$$\int_{E=0}^{\infty} \sigma(E)\phi(E)dE = \int_{v=0}^{v_{Cd}} \sigma(v)\phi(v)dv + \int_{E_{Cd}}^{E=1MeV} \sigma(E)\phi(E)dE$$

$$= n_{th}v_0\sigma_0 + \phi_{epi}\, I_0 \qquad (3)$$

Here E_{Cd} = 0.55 eV is the upper limit of energy of neutrons, which are absorbed by a 1mm thick sheet of cadmium and which is considered to be the boundary between thermal and epithermal neutrons (cadmium threshold); v_{Cd} is the corresponding velocity

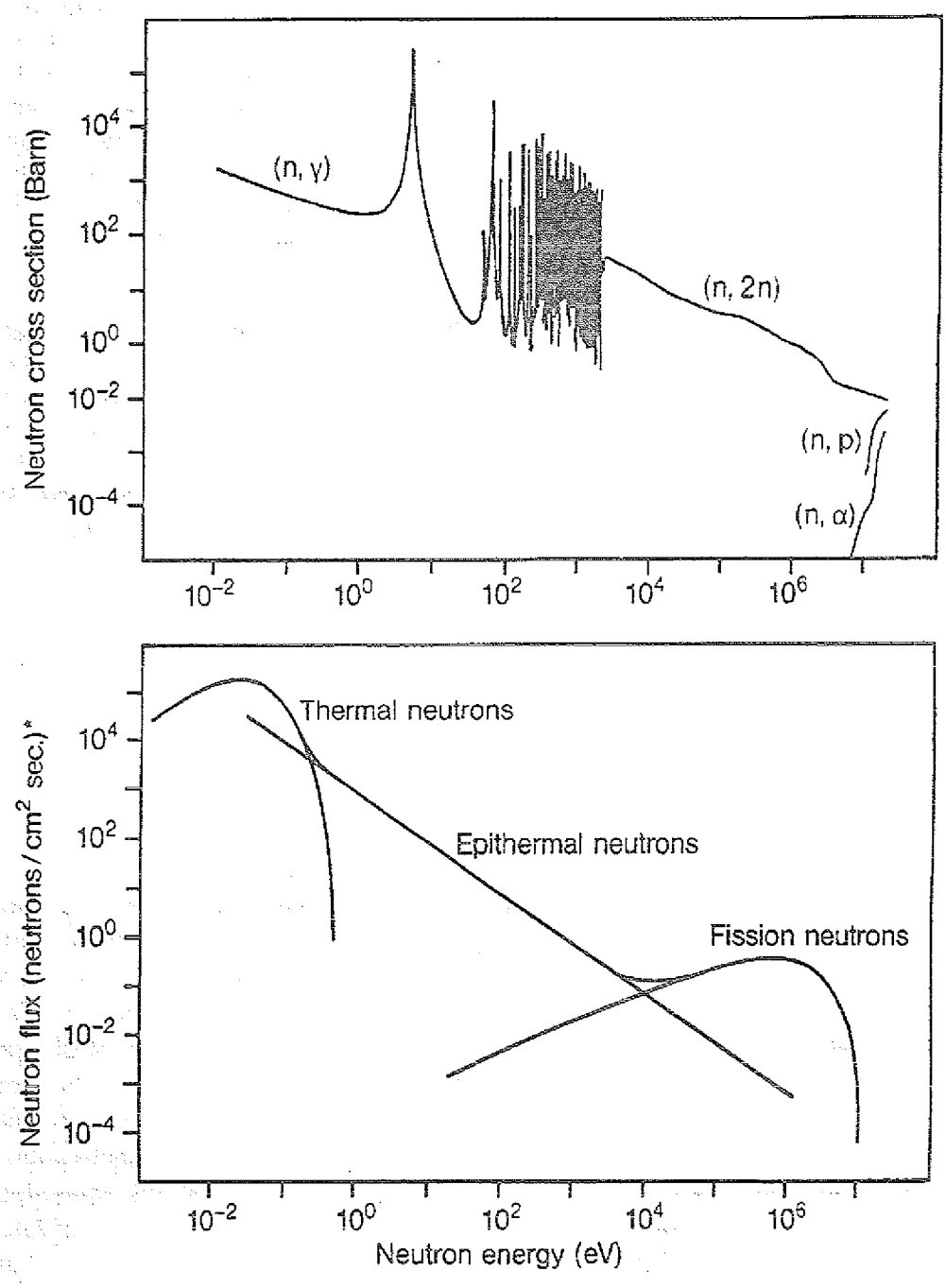

Figure 10 - Neutron cross section curve (^{197}Au as an example) and the neutron spectrum in a reactor irradiation facility.

of a neutron; 1 MeV as the upper limit is chosen because the contribution of neutrons with higher energies to the total (n,γ)-reaction rate is negligible; n_{th} is the neutron density for thermal neutrons, i.e. those with energies below the Cd cut-off; v_0 is the most probable speed of neutrons at T = 20 °C (2200 m/s) and σ_0 is the activation cross section at this speed; ϕ_{epi} is the epithermal flux and I_0 is the "infinite dilution resonance

integral". This name comes from the fact, that in the epithermal neutron region the cross section curve (Fig. 10, upper part) exhibits some discrete lines at energies, where neutrons strongly interact with atomic nuclei due to resonance effects. In a target used for the measurement of epithermal neutron cross sections these resonance neutrons will be strongly filtered out and, therefore, in the targets the atoms of the element considered must be very diluted or the targets must be extremely thin and the results have to be extrapolated to "infinite dilution".

In the following parts we want to consider the thermal and the epithermal fluxes and cross sections as effective fluxes and cross sections and use the following symbols:

$\Phi_{th} = n_{th} v_0$		thermal flux
$\Phi_{epi} = \phi_{epi}$		epithermal flux
$\sigma_{th} = \sigma_0$		thermal neutron cross section
$\sigma_{epi} = I_0$		epithermal neutron cross section
$Q_0 = \sigma_{epi}/\sigma_{th}$		cross section ratio
$Z = \frac{\lambda \exp(\lambda t_w)}{[1 - \exp(-\lambda t_i)]\,[1 - \exp(-\lambda t_m)]}$		time factor
$R_\Phi = \Phi_{th}/\Phi_{epi}$		flux ratio

The ***cross sections*** of the nuclides are constants following the conventions by which they are defined. Provided, the values of the neutron fluxes are known - one of the procedures to measure them is described in Section 11 - the amounts of elements can be calculated by

$$m = \frac{P\,M\,Z}{\eta\,h\,a\,N_A\,\sigma_{th}\,(\Phi_{th} + \Phi_{epi} Q_0)} \qquad (4)$$

In former times, the results obtained by absolute activation analysis were often found to be not very accurate. Several reasons have been responsible for that:

- The nuclear constants (σ_{th}, σ_{epi}, a, h, $t_{1/2}$) were often not accurately known.
- The accurate measurement of neutron fluxes and flux ratios was difficult and time-consuming.
- The neutron fluxes and flux ratios were not well known and, at least with medium and high-flux reactors, not constant.
- One prerequisite for the HØGDAHL-convention, the validity of the 1/E-law for the epithermal neutrons, cannot always be taken as granted.
- The 1/v-law for the thermal neutron cross sections is not valid with some few nuclides. Exceptions are, e.g., ^{151}Eu, ^{176}Lu and ^{191}Ir.

These difficulties can be overcome, as will be shown later, but had discredited the absolute method for some time.

It should be mentioned that, mainly in the early stages of the development of NAA, the absolute method has been also combined with radiochemical NAA, i.e. the radionuclide to be measured was chemically separated and counted with a β-counter. The absolute activity was then found from the β-counting efficiency and the counting rate. Such techniques are useful also nowadays, because the counting effi-

ciencies of β-counters are much higher than those of γ-ray spectrometers, so that often better sensitivities and detection limits can be attained.

3c. The relative method

It was, for a long time, the technique most often used. A standard, i.e. a known amount of the element to be determined, and the sample are irradiated together in a reactor and measured with the same counting arrangement under the same conditions. Then

$$\frac{A_{0,x}}{A_{0,s}} = \frac{m_x}{m_s} \tag{5}$$

where the subscript s stands for the standards.

All other terms of Equation (1) are identical for samples and standards. Equation (5) does not depend on how the absolute activities are measured. If they are measured with a γ-spectrometer, then it may be impractical to measure both, sample and standard, in the same counting position, because the activities of both types of samples may be very different. The efficiencies of both counting positions have to be measured and m_x can be calculated from the peak areas, P_x. Insertion of Equation (2) in (5) yields

$$\frac{P_x \eta_s \left(\frac{\lambda e^{\lambda t_w}}{1 - e^{-\lambda t_m}} \right)_x}{P_s \eta_x \left(\frac{\lambda e^{\lambda t_w}}{1 - e^{-\lambda t_m}} \right)_s} = \frac{m_x}{m_s} \tag{6}$$

where h has eliminated because it has the same value for sample and standard.

If a high resolution γ-spectrometer is used, then many elements can be determined in one sample, provided that for each element a standard has been co-irradiated. Because the measurement of many standards one after another wastes too much time and reduces the throughput of analytical samples, multielement standards have been applied. Mixtures of standard solutions have been used but more often applied are natural or technical homogeneous materials like rock ore dried plant powders, alloys, glasses etc. For convenience reference materials like the standard reference materials (SRM) of the National Institute of Standards and Technology in Washington DC (NIST) or the certified reference materials (CRM) of the International Atomic Energy Agency (IAEA) have been applied, although a number of objections were raised against such a use of these materials.

The relative method is widely applied, especially if only a few elements have to be determined in a sample, but with multielement analysis the method has some disadvantages:

- The preparation of standards for many elements can be very time-consuming, especially if each set of samples requires another combination of elements.

- Multielement standard solutions are not very stable, especially at low concentrations as they are required for an ultra-trace method like NAA. Their titers have to be checked for all elements within short intervals.
- With solid multielement standards there are problems with the homogeneity and the trace element contents are often not accurately known. This may hold even with reference materials.
- Elements not present or not analyzed in a standard material cannot be determined in the sample.
- Depending on the size and the shape of the standards prepared for irradiation they may receive other neutron fluxes than the samples and flux gradient errors occur.

3d. The single monitor or monostandard method

To overcome some of these problems, the monostandard method was introduced. It was first described by GIRARDI [9] under the name "single monitor method". Another name is "single comparator method". With this method one element, e.g. cobalt, is chosen as a standard for all elements. It is irradiated together with the samples and then counted with always the same counting arrangement. Then Equation (4) can be written with subscripts x for the element to be determined and s for the monostandard. If, additionally, the cross section ratio, Q_0, is replaced by σ_{epi}/σ_{th} and Avogadro's number is eliminated we obtain

$$\frac{m_x}{m_s} = \frac{P_x}{P_s}\,\frac{M_x}{M_s}\,\frac{Z_x}{Z_s}\,\frac{\eta_s}{\eta_x}\,\frac{h_s}{h_x}\,\frac{a_s}{a_x}\,\frac{\Phi_{th}\sigma_{th,s}+\Phi_{epi}\sigma_{epi,s}}{\Phi_{th}\sigma_{th,x}+\Phi_{epi}\sigma_{epi,x}} \tag{7}$$

With the monostandard method, there is assumed that the flux ratio Φ_{th}/Φ_{epi} is always constant so that the terms containing the fluxes can be replaced by

$$\begin{aligned}\Phi_{th}\sigma_{th,s}+\Phi_{epi}\sigma_{epi,s}&=\Phi_{eff}\sigma_{eff,s}\\ \Phi_{th}\sigma_{th,x}+\Phi_{epi}\sigma_{epi,x}&=\Phi_{eff}\sigma_{eff,x}\end{aligned} \tag{8}$$

and we can write

$$\frac{m_x}{m_s} = \frac{P_x}{P_s}\,\frac{M_x}{M_s}\,\frac{Z_x}{Z_s}\,\frac{\eta_s}{\eta_x}\,\frac{h_s}{h_x}\,\frac{a_s}{a_x}\,\frac{\sigma_{eff,s}}{\sigma_{eff,x}} \tag{9}$$

M, a, and h are constants, characteristic for each element. The same holds for σ_{eff} as long as the flux ratio remains unchanged. These constants can be combined to a complex constant:

$$k_{e,x} = \frac{M_x}{M_s}\,\frac{h_s}{h_x}\,\frac{a_s}{a_x}\,\frac{\sigma_{eff,s}}{\sigma_{eff,x}} \tag{10}$$

so that

$$\frac{m_x}{m_s} = k_{e,x}\,\frac{P_x}{P_s}\,\frac{Z_x}{Z_s}\,\frac{\eta_s}{\eta_x} \tag{11}$$

To practice the monostandard method in a laboratory, it is necessary to determine the k_e-factors for all elements or, to say it more accurate, for all relevant γ-lines of

activation products expected by thermal neutron activation. Because these factors are valid only with the experimental setup for which they are measured, they are marked here by the subscript *e* for experiment. In some laboratories the counting of samples was always done with the same geometry, i.e. that the ratio η_s/η_x remained constant and could be included in the k_e-factors.

As soon as another irradiation position is used (or if the counting geometry has to be changed) the whole set of several hundred k_e-factors has to be remeasured. This inflexibility makes the monostandard method somewhat impractical. But these restrictions are not as stringent as they seem to be at a first glance: The contribution of the epithermal neutrons to the activation is usually small and shifting from one irradiation facility to another one will cause only small errors except with some elements having high cross section ratios. Such small errors have been tolerated as long as more accurate methods of trace element analysis were not available. But meanwhile other methods have attained similar detection limits and good accuracies, and analytical problems have become important, which require good accuracies also with low contents of trace elements.

3e. The Gent k_0-standardization method

For a more accurate calculation of analytical results the concept of effective cross sections for a reactor neutron spectrum is not suitable and the activation by thermal and epithermal neutrons has to be treated separately as it is already outlined in the Section "Neutron fluxes and cross sections". By this way it was also possible, to apply analytical constants, which are independent from the experimental conditions in a laboratory. To omit the effective flux and cross section we have to return from Equation (11) to Equation (7) and to re-introduce $Q_0 = \sigma_{epi}/\sigma_{th}$. The Equation reads now

$$\frac{m_x}{m_s} = \frac{P_x}{P_s}\,\frac{M_x}{M_s}\,\frac{Z_x}{Z_s}\,\frac{\eta_s}{\eta_x}\,\frac{h_s}{h_x}\,\frac{a_s}{a_x}\,\frac{\sigma_{th,s}}{\sigma_{th,x}}\,\frac{\Phi_{th}+\Phi_{epi}\,Q_{0,s}}{\Phi_{th}+\Phi_{epi}\,Q_{0,x}} \qquad (12)$$

The constant factors outside the terms containing the fluxes can be combined to obtain a complex constant:

$$k = \frac{M_x}{M_s}\,\frac{h_s}{h_x}\,\frac{a_s}{a_x}\,\frac{\sigma_{th,s}}{\sigma_{th,x}} \qquad (13)$$

Such k-values can be calculated from the nuclear constants involved, but as long as the values of these constants are not accurately known the same errors will occur as were described with the absolute method. Therefore DE CORTE, SIMONITS, MOENS et al. have measured such factors for nearly all important (n,γ)-activation reactions or, to say it more precise, for the strong γ-lines of the resulting activation products. They used gold (^{197}Au) as a standard or reference nuclide, because its nuclear constants are very accurately known. In their concept the reciprocal value of Equation (13) is defined as the analytical factor:

$$k_{0,x}^{Au} = \frac{M_{Au}}{M_x}\,\frac{h_x}{h_{Au}}\,\frac{a_x}{a_{Au}}\,\frac{\sigma_{th,x}}{\sigma_{th,Au}} \qquad (14)$$

To apply the k_0-standardization method, it is not necessary to use always gold as a standard nuclide. Any other nuclide can be used as a standard, if its k_0^{Au}-value is known. Then the amount of an element is calculated by

$$m_x = m_s \frac{P_x}{P_s} \frac{Z_x}{Z_s} \frac{\eta_s}{\eta_x} \frac{k_{0,s}^{Au}}{k_{0,x}^{Au}} \frac{\Phi_{th} + \Phi_{epi} Q_{0,s}}{\Phi_{th} + \Phi_{epi} Q_{0,x}} \tag{15}$$

or

$$m_x = m_s \frac{P_x}{P_s} \frac{Z_x}{Z_s} \frac{\eta_s}{\eta_x} \frac{k_{0,s}^{Au}}{k_{0,x}^{Au}} \frac{R_\Phi + Q_{0,s}}{R_\Phi + Q_{0,x}} \tag{16}$$

With these Equations, besides of the $k_{0,x}^{Au}$-values, the γ-peak areas, the peak counting efficiencies and the time factors have to be determined for the analyte and the standard, and the flux ratio must be known. If a reactor with a stable flux ratio is used it may be sufficient to measure it only once within long periods, and with each actual irradiation only the thermal flux has to be measured. In such a case, gold can be used as a standard and then $k_{0,s}^{Au} = k_{0,Au}^{Au} \equiv 1$.

3f. The k_0-method as it is applied in the Radioanalytical Section of the ZCH

The practice of measuring only the thermal neutron flux, as described in the last chapter, is not suitable with high-flux reactors like the FRJ-2 here in Jülich, where the flux ratio changes during an operation period according to the fuel burn-up and the corresponding movement of the control rods. Therefore, in our laboratory zirconium is used as a standard or flux monitor.[11] It forms two isotopes, ^{95}Zr and ^{97}Zr. The Q_0-values of the two reactions are quite different, so that with one wire or foil the two fluxes, Φ_{th} and Φ_{epi}, can be determined. Writing Equation (4) for ^{95}Zr with subscripts 5 and resolving for the thermal flux we get

$$\Phi_{th} = \frac{P_5 M_5 Z_5}{\eta_5 h_5 a_5 N_A \sigma_{th,5} m_5} - \Phi_{epi} Q_{0,5} \tag{17}$$

Because we want to use the k_0-factors instead of the nuclear constants we replace, according to Equation (14)

$$\frac{M_5}{h_5 a_5 \sigma_{th,5}} = \frac{1}{k_{0,5}^{Au}} \frac{M_{Au}}{h_{Au} a_{Au} \sigma_{th,Au}} \tag{18}$$

so that

$$\Phi_{th} = \frac{P_5 Z_5}{k_{0,5}^{Au} \eta_5 N_A m_5} \frac{M_{Au}}{h_{Au} a_{Au} \sigma_{th,Au}} - \Phi_{epi} Q_{0,5} \tag{19}$$

The same equation can be written with subscript 7 for ^{97}Zr. If a zirconium wire is irradiated as a monostandard or a flux monitor, then the flux is the same for both isotopes and $m_5 = m_7 \equiv m_{Zr}$

$$\frac{P_5 Z_5 C_{Au}}{k_{0,5}^{Au} \eta_5 m_{Zr}} - \Phi_{epi} Q_{0,5} = \frac{P_7 Z_7 C_{Au}}{k_{0,7}^{Au} \eta_7 m_{Zr}} - \Phi_{epi} Q_{0,7} \tag{20}$$

where C_{Au} replaces the expression $M_{Au}/h_{Au} a_{Au} \sigma_{th,Au} N_A$. The thermal and the epithermal flux can then be calculated from the peak areas of the γ-lines of the two zirconium isotopes by

$$\Phi_{epi} = \frac{C_{Au}}{m_{Zr}(Q_{0,5} - Q_{0,7})} \left(\frac{P_5 Z_5}{k_{0,5}^{Au} \eta_5} - \frac{P_7 Z_7}{k_{0,7}^{Au} \eta_7} \right) \tag{21}$$

$$\Phi_{th} = \frac{C_{Au}}{m_{Zr}(Q_{0,7} - Q_{0,5})} \left(\frac{P_5 Z_5 Q_{0,7}}{k_{0,5}^{Au} \eta_5} - \frac{P_7 Z_7 Q_{0,5}}{k_{0,7}^{Au} \eta_7} \right) \tag{22}$$

Finally, the amount of an element can be calculated from the corresponding peak area by

$$m_x = \frac{C_{Au} P_x Z_x}{k_{0,x}^{Au} \eta_x (\Phi_{th} + \Phi_{epi} Q_{0,x})} \tag{23}$$

3g. Analysis with isotope-related analytical factors (k_i)

k_0-factors are analytical factors related to single γ-lines and, consequently, Equation (23) is applicable only with well resolved γ-lines in a γ-spectrum. But there are situations, where neither the γ-spectrometer nor the computer program for the evaluation of γ-spectra can resolve overlapping or superposed peaks. GUNNINCK and NIDAY [12] have proposed a procedure to unfold such peak clusters. It uses not only the energies but also the intensities of the γ-lines as characteristic parameters and calculates absolute activities of the radionuclides. Absolute activities are also obtained, when radiochemical activation analysis is carried out and the separated nuclides are measured with a β-counter with known counting efficiency.

The γ-ray-related k_0-factors are not suitable to calculate amounts of elements from absolute activities and isotope-related analytical factors are preferable. They can be calculated from the k_0-factors by dividing them through the γ-ray abundances and eliminating the nuclear constants of gold.

$$k_i = C_{Au} \times \frac{\sum_j \frac{h_j}{k_{0,j}^{Au}} w_j}{\sum_j w_j} \tag{24}$$

where j is the number of k_0-factors known for one nuclide and w_j is a weighing factor considering the errors of k_0- and h-values. f_{k_0} and f_h mean relative errors.

$$w_j = \frac{k_{0,j}^{Au2}}{h_j^2 \, (f_{k_{0,j}}^2 + f_{h_j}^2)} \tag{25}$$

The γ-ray abundances, h, can be taken from relevant compilations, i.e. [6,13,14], and for the γ-lines for which k_0-values have been measured, γ-ray abundances are also listed in the tables of DE CORTE et al.[10]. For nuclides, where k_0-factors have not been measured, k_i-factors can be calculated directly from the nuclear constants,

$$k_{i,x} = \frac{M_x}{N_A \, a_x \, \sigma_{th,x}} \tag{26}$$

but these values are not as reliable as those obtained from the k_0-factors. k_i-values are listed, together with other nuclear data, in Table 7. With k_i-factors results are calculated by

$$m_x = \frac{A_x \, k_{i,x} \, Z_x}{\Phi_{th} + \Phi_{epi} \, Q_{0,x}} \tag{27}$$

where

$$\Phi_{epi} = \frac{A_5 \, k_{i,5} \, Z_5 - A_7 \, k_{i,7} \, Z_7}{m_{Zr} \, (Q_{0,5} - Q_{0,7})} \tag{28}$$

and

$$\Phi_{th} = \frac{Q_{0,5} \, A_7 \, k_{i,7} \, Z_7 - Q_{0,7} \, A_5 \, k_{i,5} \, Z_5}{m_{Zr} \, (Q_{0,5} - Q_{0,7})} \tag{29}$$

3h. Return to the absolute method

With Equation (27) we use absolute decay rates, absolute flux values and analytical factors, which are composed of nuclear constants. The absolute decay rates are obtained by measurements with calibrated instruments. In the case of γ-spectra, the calibration factors depend on the γ-energy, and the calibration curves are measured with a set of calibration standards, which are calibrated samples of radionuclides. These radionuclides are usually not the same as those which are measured in the analytical samples.

This procedure is, formally, similar to that of gravimetry, where an analytical preparation, e.g. a precipitate, is weighed with a calibrated balance and the amount of the element to be determined is calculated using a gravimetric, i.e. an analytical factor, which is a complex constant composed of atomic weights and stoichiometric numbers. The calibration of the balance is done with a set of calibrated weights which are not of the same material as the precipitate weighed. Thus, if we consider gravimetry as an absolute analytical method, we have to concede that also to the absolute method of activation analysis: With both methods analytical procedures can be standardized without using elemental standards; they are based on basic analytical constants and require calibrated instruments to be carried out. The term absolute does not mean, that the method is inherently accurate ore especially precise. Indeed,

with activation analysis the procedure and the analytical instruments used, the γ-spectrometers, are much more complicated and the analytical constants are not as accurate known as it is true for gravimetry.

Starting from Equation (1) and going through the chapters of single monitor and k_0-method we have returned to the absolute method, but it was not like going round in a circle but more like following the turn of a screw. The gain in accuracy, we have attained, is due to the introduction of the k_0-factors of DE CORTE et al. These data, measured carefully and with analytical precision have replaced the often inconsistent sets of nuclear constants formerly used with absolute activation analysis. By the last step towards absolute activation analysis, the introduction of the k_f-factors and splitting off the γ-ray abundances, h, from the k_0-factors, some slight inconsistency has, indeed, be reintroduced. However, an investigation in our laboratory, still unpublished, has shown, that k_f-factors calculated from nuclear data (taken from some recently published and independent compilations) by Equation (26) and those calculated from k_0-factors by Equation (24) are usually within the errors of the k_0-factors, i.e. the calculated values confirm the accuracy of the k_0-values of DE CORTE et al. and give security with the application of k_f-factors.

3i. The treatment of non-1/E epithermal neutron spectra

Out of the drawbacks formerly connected with absolute NAA and listed after Equation 4 the first three have been overcome by the introduction of the k_0-factors. and the measurement of neutron fluxes with double flux monitors like zirconium. But errors due to non-1/E epithermal neutron spectra and non-1/v thermal neutron cross sections have not yet been considered in this lecture. These problems have also been investigated by DE CORTE et al. during the development of the k_0-method and presented in a number of publications which are comprehended in Ref.[15]. As has first been outlined by HÄFELE [16] in a real reactor the shape of the epithermal neutron spectrum can be described by $d\phi/dE \propto 1/E^{1+\alpha}$, where α is a small number, usually between -0.05 and +0.15. The resonance integrals, I_0, (or in our notation epithermal cross sections, σ_{epi}), and consequently the cross section ratios, Q_0, are, by definition, constants only if $d\phi_{epi}/dE \propto 1/E$, i.e. if $\alpha = 0$. Otherwise they depend on α and, following DE CORTE et al. [15], we can write

$$Q_0(\alpha) = \frac{Q_0 - 0.429}{\overline{E_r}^{\alpha}} + \frac{0.429}{(2\alpha + 1) \times 0.55^{\alpha}} \qquad (30)$$

where the first term refers to the resonance lines in the cross section curve (Fig. 10) and the second term to the epicadmium-tail (i.e. above 0.55 eV) of the 1/v-cross section curve. $\overline{E_r}$ is the effective resonance energy [17]. Calculated values are inserted in the tables of DE CORTE et al. [10], and some more recent values in Ref..[18]. For the measurement of α-value s in irradiation facilities several procedures have been proposed requiring the irradiation of three or more elements (flux monitors) with and without cadmium shieldings and calculating the α-values from the activities.[15,19] If $\alpha \neq 0$ then $Q_0(\alpha)$-values have to be calculated from the Q_0-values using Equation (30) and used instead of them to calculate neutron fluxes (Equations 21 and 22) and analytical results with k_0-factors (Equation 23) or with k_f-factors (Equation 27).

4. The accuracy and traceability of activation analysis.

Activation analysis was for a long time considered as the most sensitive method of trace element analysis, which was true at least for a great number of elements. Meanwhile some other techniques have been introduced capable to compete with it. Furthermore, activation analysis was said to yield inherently accurate results. This repute was mainly based on the facts that it requires a minimum of sample handling and therefore avoids the risk of contaminating the samples, and that, independent of the technique used, the theoretical basis is well understood and the procedures and effects leading from the analytical signal to the calculation of the results can be quantitatively described as has been shown with the equations above. In reality, however, it had often to be noticed, that results obtained by NAA not always fulfilled these expectations. An example has been impressively outlined by SMALES.[20]

> He compared the results of several methods which had been used in the elemental analysis of moon samples from the Apollo-II mission. His table of analytical methods for minor and trace elements (the "minor leagues") is shown here in Table 2. It includes also atomic absorption spectrometry and spark source mass spectrometry, which he had omitted. Indeed, NAA has contributed more results than all other methods together and in this respect it seemed very successful. But only 54% of the results were accurate within $\pm 10\%$, and therefore NAA had to be sent to the lower ranks. One might try to explain such bad results of neutron activation analysis by the state of the art at that time. During the late sixtieths a great number of activation analyses were still carried out by radiochemical techniques, which require experience and skilful working. High-resolution γ-ray spectrometry was a comparably new technique and some of its problems were not yet completely understood in all laboratories. But also with round robbins carried out recently, e.g. with analyses carried out to characterize candidate materials for analytical reference samples of the BCR of the European Community, activation analysis came out badly.
>
> However, one can also find other, contrary experiences. MARKERT [21] wanted to analyze biological samples for an "environmental cadaster" and used standard reference materials, Citrus leaves (NIST-SRM 1572) and Pine needles (NIST-SRM 1575), to check the accuracy of the procedures. He applied different analytical methods to compare the accuracy, the applicability and the economy of the methods. The analyses were partially carried out by himself in our laboratory and partially by other analysts in specialized laboratories abroad. For NAA he applied the k_0-method as it is installed and used routinely in the Radiochemical Section of the ZCH/KFA. The results are comprehended in Table 3. The lowest deviations from the certified values - in the mean - were found with the results obtained by INAA. The largest number of elements could be detected by ICP-OES with chemical separation of the rare earth elements. But looking to 24 elements considered to be important in environmental research - essential and toxic elements and those which can be used as guiding elements - then activation analysis delivered the most results, although Cd and Pb, which for a long time seemed to be the most relevant "toxic elements", cannot be detected with high sensitivity and were not found.

Such examples, good or bad, must not be overemphasized and generalized. What we should keep in mind is, that a method is not accurate or inaccurate *per se*, but that depends on how it is carried out. Some methods, however, include a number of dif-

Table 2 - Accuracies of methods for trace elements
Ranking in the "Lunar minor leagues"
(*after SMALES* [20])

Method	Total number of results	'Errors'	Batting average (%)
MS-ID	42	0	100
XRF	24	10	58
AA	115	53	54
OES-Arc	26	18	31

MS-ID = Isotope dilution mass spectrometry, XRF = x-ray fluorescence spectrometry, AA = activation analysis (not specified, but mainly reactor NAA with and without radiochemical separations), OES-Arc = arc emission spectrography

Table 3 - Instrumental multielement methods of trace element analysis
Another comparison of their accuracies (*after MARKERT* [21])

Method	Mean number of elements determined	Mean of deviations from certified values (%)
INAA(k_0)	19	12
OES-ICP	14	23
OES-ICP(Lan)	28	40
XRF	11	43
MS-ICP	12	53

INAA(k_0) = INAA with the k_0-method as described above, OES-ICP = Optical emission spectroscopy with inductively coupled plasma, OES-ICP(Lan) = OES-ICP with chemical separation of the rare earth elements, XRF = x-ray fluorescence spectrometry, MS-ICP = Mass spectrometry with ICP.

ficult working steps. Others are difficult to standardize, i.e. they require standards of approximately the same composition as the sample itself. These are not always available. As has already been outlined, with absolute INAA many of these drawbacks are not pertinent. But there remain several possible sources of errors, which have to be considered.

4a. Types of error

We want to differentiate between three types of error the analyst has to deal with:

- accidental errors
- systematical errors
- random errors

Typical ***accidental or handling errors*** are:

- Confusion of samples
- Use of an old standard solution whose titer has changed.
- False noting down of measured data, e.g. sample weight or counting time; misplacing a decimal point.

There is no regularity in the occurence of accidental errors and it is not possible to estimate the extent of their influence on the error of an analytical result. Provisions can be made to avoid such mistakes and automatization of analytical procedures can help to minimize their occurence. But anywhere there remain "interfaces" between the analyst and his or her equipment.

Systematical errors of analytical results will occur, if always the same mistake is done with a procedure.

> Such an error, e.g. would occur when the relative method is used and the standard is always placed in the lower part and the sample is placed in the upper part of an irradiation capsule. Due to the flux gradient the element contents found will have always the same relative error, and this holds for all elements. Another example shall be taken from the area of γ-ray spectrometry: If the influence of γ-γ-coincidences on the peak counting yields are not considered, systematic errors will occur only for certain elements. Their sizes will be different from element to element.

It is the aim of the following chapters to outline all sources of systematical errors. To a large extent they can be avoided by an appropriate choice of the experimental equipment and careful control of its setups. In many cases correction factors can be calculated or experimentally determined. However, because analytical samples consist usually of different materials and have different sizes and shapes, it is practically not always possible to bring all systematical errors to zero. We shall see, that all parameters required to calculate analytical results from the experimental data are afflicted with uncertainties, which we can consider as "randomized systematical errors". Estimations of these errors will be given. Strictly speaking these errors have the meaning of the standard deviations of a normal distribution, but since only rough estimates are possible and often the normal distribution is not strictly valid or proved, it is not necessary to give here a more precise definition of what the word "error" means in this context. In every case we treat these errors as if they were of random nature and the error propagation law is applicable.

Doing so, there is obviously no principal distinction between these randomized systematical error and ***random errors***. The statistical counting error can be considered as such a true random error and it is obviously the only one with NAA. The possibilities of reducing the statistical counting error are limited. The counting time cannot advertently extended and the reduction of the error is less than proportional to its inverse square root. The improvement of the counting efficiency, e.g. by reducing the distance between sample and detector, will increase the uncertainties of geometrical or coincidence counting errors.

Consequently, all efforts to get accurate results have to deal with the systematic errors. They have to be minimized and randomized for all the different types of samples. If one optimizes a procedure for a certain type of samples, then the randomized systematical error will become smaller.

In the following Sections the different sources of systematical errors shall be investigated. The uncertainties of the parameters in the activation equation have different effects on the total error of the analytical result according to the error propagation law. As an example, the sources of error influencing determinations by the absolute method with k_i-factors (Equation 27) shall be investigated. The square of the relative error of the amount of element to be determined is

$$f_m^2 = \frac{s_m^2}{m^2} = \frac{s_A^2}{A^2} + \frac{s_{ki}^2}{k_i^2} + \frac{s_Z^2}{Z^2} + \frac{s_\Psi^2}{\Psi^2} \tag{31}$$

where s are the absolute errors or uncertainties of the indicated parameters. The subscripts x are omitted. Ψ is the term containing the fluxes, $\Psi = \Phi_{th} + \Phi_{epi} Q_\alpha$, and Z is the time factor as defined before Equation (4). Q_α will be used as a short form of $Q_0(\alpha)$ (see Equation 30).

4b. Sources of error with the measurement of the activities

The activities, A, are measured via the peak areas, $A = P/h\,\eta$, and their errors are composed of those of P, h and η. With most nuclides more than one peak is available and the activity is calculated by

$$A = \frac{\sum_j \frac{w_j P_j}{\eta_j h_j}}{\sum_j w_j} \tag{32}$$

where w_j are weighing factors

$$w_j = \frac{1}{\left(\frac{s_{P,j}}{P_j}\right)^2 + \left(\frac{s_{\eta,j}}{\eta_j}\right)^2 + \left(\frac{s_{h,j}}{h_j}\right)^2} \tag{33}$$

and the error of A is

$$s_A = \frac{1}{\sqrt{\sum_j w_j}} \tag{34}$$

The sources of errors affecting that of the peak area are summarized in Table 4.

Typical effects of errors due to self-coincidence, to counting geometry and to γ-ray self-absorption are illustrated in Figures 11 ,12 and 13.

To understand the self-coincidence (or sum- or γ-γ-coincidence) error we assume a decay scheme as it is shown in the right upper corner of Figure 11. 40% of the events populating the 600 keV level decay immediately to the ground state, 60% form a triple cascade. All four γ-lines are seen in the γ-spectrum. If a photon of the 600 → 300 keV transition is emitted, then the chance to cause a detector output pulse is $\eta_{T,300}$, the total counting efficiency for a 300 keV photon. This pulse may be caused by a photoeffect; then the output pulse corresponds to the full energy of the γ-photon. It contributes to the formation of the γ-line in the spectrum and this chance is $\eta_{P,300}$. Or the pulse is caused by some scattered photon - backscattered in the surroundings of the detector or compton scattered inside the detector - and the output pulse is smaller than that of a photoeffect or another full-energy event and it does not contribute to the γ-line but to the background continuum left of the line.

At the same time as the 300 keV photon the two photons of the 300 → 100 and of the 100 → 0 keV transitions are emitted and have their chances to be detected, $\eta_{T,200}$ or $\eta_{P,200}$ and $\eta_{T,100}$ or $\eta_{P,200}$. If any 100 or 200 keV photon meets the detector at the same time as a full-energy event of a 300 keV photon has occured, then the output pulse of the detector corresponds to the sum of the energies absorbed from the 300-keV- and the other photons, i.e. the pulse does not contribute to the full energy peak. The true chance for a photon emitted in a cascade to be detected in the full energy peak is consequently

$$\eta_{300} = \eta_{P,300}(1 - \eta_{T,200})(1 - \eta_{T,100}) \tag{35}$$

and the same holds correspondingly for the two other lines.

If all three photons are detected at the same time by full energy events, then the sum of the charges created corresponds to that of a 600 keV photon. Such events increase the intensity of the full energy peak:

$$\eta_{600} = \eta_{P,600} + \eta_{P,300}\,\eta_{P,200}\,\eta_{P,100} \tag{36}$$

The errors are

$$\frac{f\eta_E}{\eta_E} = \frac{\eta_{P,E}}{\eta_E} - 1 \tag{37}$$

They become larger with increasing η, i.e. if the sample - detector distance is reduced or if a larger detector is used. They depend on the efficiencies of the γ-lines considered, those of the other lines in the cascade and the number of lines in a cascade. One γ-line can be found in more than one cascade, according to branching ratios. X-rays emitted during the radioactive decay are also in coincidence with the γ-rays and have to be included in a calculation of the correction. Such a computer program has been developed by L. MOENS (University of Gent, Institut of Nuclear Sciences). The program treats also errors of γ-ray self-absorption and geometrical errors due to different sam-

Table 4 - Contributions to the error of the activity.

Peak area, P

- **Statistical counting error** **2 - 10 %**
  Is usually calculated with the γ-spectrum evaluation procedure. Includes uncertainties of the determinations of the peak area and of the background. In optimal cases it may be <0.1%. Usually it is 1 to 5 % and with weak peaks the size of the error is unlimited, but errors >50% are with peaks near to the limit of detection and these should not be considered with analyses.

- **Errors of the peak evaluation program** **0.2 - 2 %**
  Free peaks are accurately evaluated with present day's computer programs. Problems may occur with superimposed lines and high errors may remain undetected if the results of the peakfit procedure are not carefully checked. This can be done by checking the χ^2 values or by visual inspection of the peaks and the fitted curve on the screen, which is possible with many γ-spectrum evaluation programs.

- **Dead time errors**
  They will be treated with the error of the time dependent term, Z.

Counting efficiency, η

- **Error of the calibration source** **2 %**
  Errors with radioactive reference samples are mostly 1.5 - 2 %. This holds for solid sources (disk and point sources) as well as for solutions. With some nuclides errors are up to 3%. If solutions are used to prepare samples with certain shapes and volumes, then some additional error is introduced by dilution and aliquotation. The error will be ruled out if measuring positions for samples and standards or flux monitors are calibrated with the same source.

- **Error of the efficiency calibration curve** **0.5 - 2 %**
  Includes precision of measured points and the quality of the fitted curve. Sum-coincidence errors are not included; they have to be corrected for, e.g. if ^{152}Eu is used as calibration source.

- **Geometrical errors** **0.5 - 2 %**
  A typical case is the measurement of a set of samples having more or less the same size and shape. It is not practical to measure the counting efficiency curves for each individual sample. Instead of that, a calibration source with the size, the shape and the density of a "typical sample" is used and for for all real samples slight deviations will appear. Depending on the sample - detector distances the uncertainties are 0.5 - 2 %. In unfavorite cases, e.g. if samples with irregular shapes have to be measured in positions near the detector, errors of ≃10% must be admitted. Such large errors may also occur, if no geometry correction is carried out (See Fig. 12).

(continued on next page)

Table 4 - Contributions to the error of the activity (continued)

***Counting efficiency*, η** (continued)	
◦ **γ-ray self-absorption** *In optimal cases (hard i.e. high-energy γ-rays, thin samples) the error is <0.1%. With typical samples it will be 0.5 - 2 %, depending on the γ-ray energy, if appropriate corrections are made. If large and irregular shaped samples have to be measured, the error may be 2 - 5 %. Without corrections errors of 20 - 30 % will occur (see Figure 13)*	**0.5 - 2 %**
◦ **γ-γ-coincidences** *They can be strongly reduced - as it is true with the geometry errors - if large sample - detector distances (> 10 cm with ≃ 100 cm^3 detectors) are chosen. Then typical values will be 0 - 2 %. Otherwise, if no automatical correction is included in the γ-spectrum evaluation procedure, the correction by separate calculations is difficult and therefore usually not carried out. Then errors up to 30 % may occur (see Figure 11)*	**0 - 2 %**
γ-ray abundances, h *see Table 6*	**2 - 5 %**
Error of the activity, A *Includes all errors described except the statistical error. Higher errors may occur but are avoidable by careful minimization of all sources of error. The lower limit is mainly determined by the error of the γ-ray abundance. Where its uncertainty is <2%, smaller errors are attainable.*	**1 - 5 %**

ple shapes. It is intended to be installed on the μ-VAX-II in our laboratory but is not yet included in the automatic computer procedure for the calculation of results with k_f-factors.

The curves of Figure 11 shall convey an impression on the size of γ-γ-coincidence effects. The effects of pulse losses according to Equation (35) are much larger than those of the addition of pulses according to Equation (36), because $\eta_P \leq \eta_T$. A table with examples for several nuclides can be found in Ref. [22]

Geometrical counting errors have always to be considered if samples of different size and shape have to be measured, because not for each individual sample a calibration sample with the same dimensions can be prepared. The problem has also to be considered with the relative method of NAA, because standard or reference samples are usually different in size, shape and density from the analytical samples.

With Figure 12 it is assumed that both, sample and standard, are cylinders of 10 mm diameter and the standard is 1 mm and the sample is 10 mm thick. Both specimens are

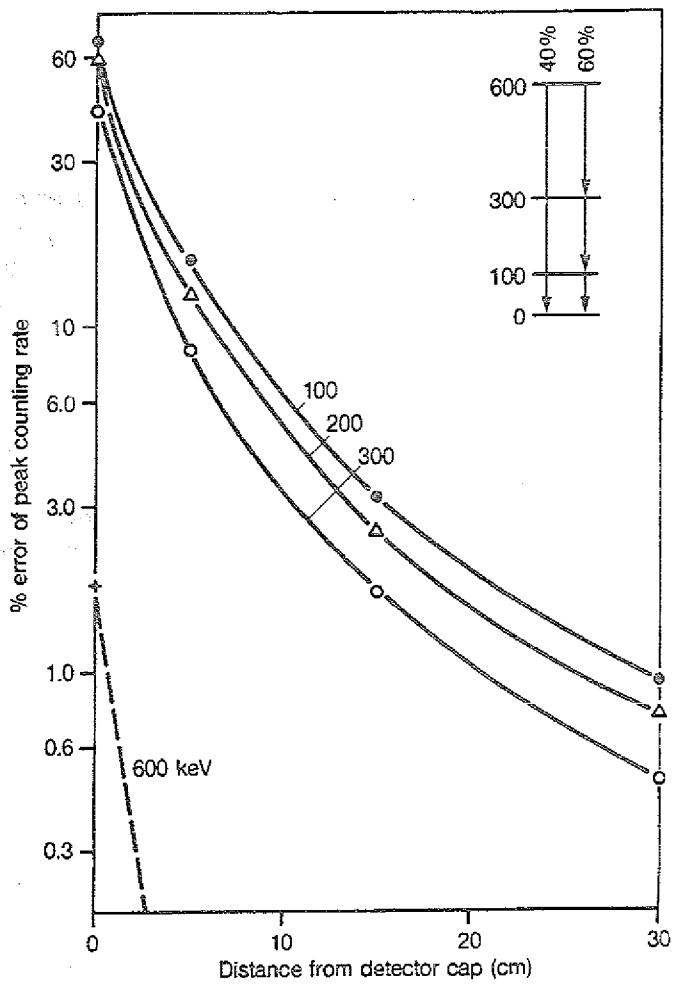

Figure 11 - Errors due to γ-γ-coincidences, calculated for a (hypothetical) decay scheme shown in the right upper corner. The errors are calculated by Equations (35) and (36). The example is valid for a 115 cm^3-detector (relative efficiency 28%).

measured in the same position. Then the counting error depends on the sample - detector distance as shown.

The correction of geometry errors for samples of regular shape and being not too large, is included in the program of MOENS mentioned above.

Another source of errors is ***γ-ray self-absorption*** (self-shielding, self-attenuation). A rule of thumb says, that hard γ-rays are practically not absorbed in small specimens of a few grams, i.e. of the size of analytical samples, and that samples consisting of light elements like water or biological matter, do not strongly attenuate γ-rays. But this rule is not applicable to accurate measurements of good, analytical quality, as can be seen from Figure 13. Even γ-rays of 500 keV are absorbed to 4 - 5 % in samples of thickness 1 g/cm^2, and this factor is nearly independent of the composition of the sample.

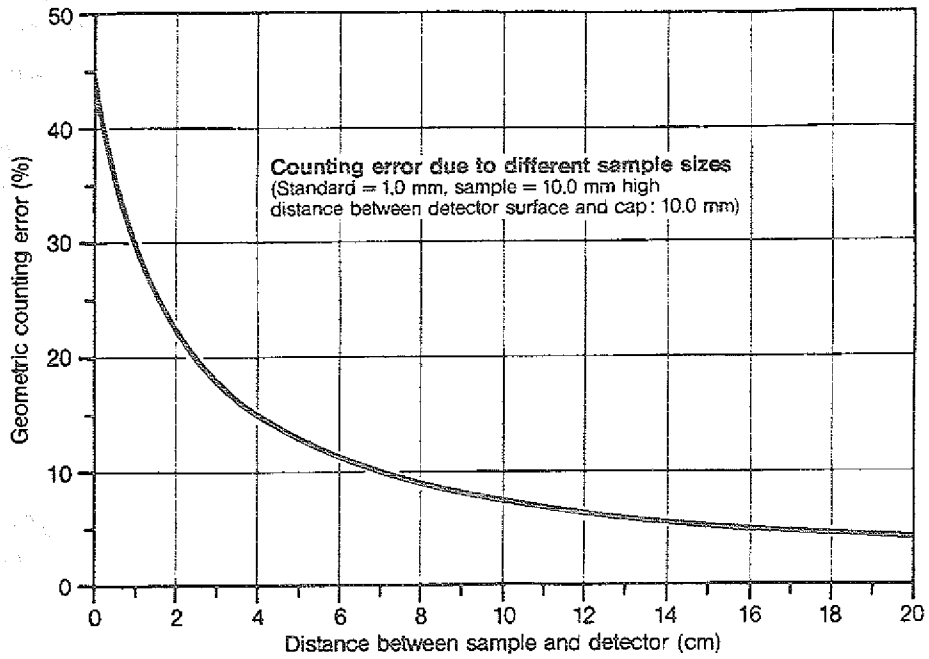

Figure 12 - Geometrical error if samples of different size are measured in the same positions. Distance 0 is 10 mm from the detector surface, because of the distance between detector and cap, the thickness of cap and that of the sample holder.

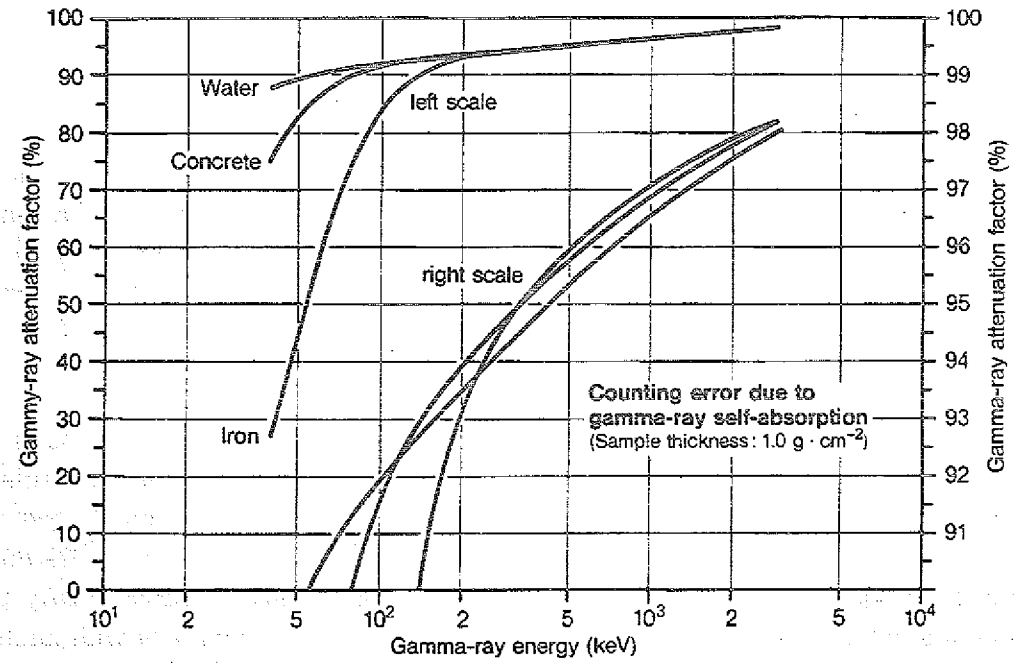

Figure 13 - Counting error due to γ-ray self-absorption.
Note different scales right and left.

As a result of the estimations of errors involved in the determination of the activity, A, (Table 5) we can state that, because analytical samples are usually far from being ideal counting samples with respect to size, shape, density and activity, it will be very hard to obtain accuracies better than 3% for their activities. With the flux wires or foils the situation is better. Their size and thickness is small, they contain only two nuclides, the γ-ray abundances are known to $\pm 0.4\%$ or better, and the peaks to be evaluated do not overlap. Their amount can be made so that the activities generated are optimal for the counting position to be used and, therefore, errors of the activities can be kept $<0.5\%$.

4c. The accuracies of k_f-factors and other nuclear constants (h, k_0, Q_0, $\bar{E}_r$, η, λ)

k_f-factors are calculated from k_0-factors and from γ-ray abundances. Therefore, these two types of data have to be discussed with respect to their uncertainties. Additionally, Q_0-values, effective resonance energies, $\bar{E}_r$ and the decay constants, $\lambda = \ln 2/t_{1/2}$, and their errors have to be known for the calculation of results.

k_0-factors have been measured by DE CORTE et al.[10]. Recently some additional values have been measured [23] and further k_0-factors were calculated from the nuclear data by Equation (14). These data are included in a data base used in the ZCH for neutron activation analysis. Table 5 gives a review of their accuracies.

The traceability of the k_0-values is usually good, because their measurement and the sources of the data used are thoroughly described in Ref.[15] and some recent publications reviewed in Ref.[23].

With ***γ-ray abundances*** we find uncertainties as they are listed in Table 6. The data are taken from the data base mentioned above containing 479 γ-lines of 143 radionuclides useful in activation analysis. In the upper row is shown, how many γ-ray abundances have uncertainties within the indicated levels. In the second row only the γ-lines with the lowest errors of each radionuclide are considered, because these errors will mainly determine the errors of the k_f-factors calculated by Equation (24).

The errors of γ-ray abundances have two components. γ-Ray abundances are measured with γ-ray spectrometers. The relative intensities of the γ-lines - relative to the most abundant or another prominent line - can usually be measured with higher accuracy than the absolute activities of the nuclides, because absolute counting - e.g. by a 4π-β- or a β-γ-coincidence counting technique - requires very pure radionuclides, which are often difficult to prepare. This holds especially with nuclides having branched decay schemes with members of similar half-lives. Consequently, γ-ray abundances have often a large systematical, isotope-related, and a low γ-ray-related error. With the calculation of k_f-factors by Equation (24) total errors of the γ-ray abundances are considered (see Equation 38). More accurate data of γ-ray abundances are desirable with many nuclides in order to get more accurate analytical k_f-factors.

Table 5 - Accuracies of k_0^{Au}-values [a]

Ranges of errors	≤0.5 %	0.5 - 2 %	2 - 5 %	> 5 % [b]
Number of reactions whose best k_0-factor falls in the indicated error range	29	72	1	41
Number of γ-lines, whose k_0-factors fall in the indicated error range	43	231	5	200

[a] Most data are from DE CORTE et al.[10, 23] Some few are calculated by Equation (14); their errors are assumed to be >5%. [b] Including "not recommended" k_0-values.

Table 6 - Accuracies of γ-ray abundances

Ranges of errors	≤0.5 %	0.5 - 2 %	2 - 5 %	> 5 %
Number of reactions whose most accurate γ-line falls in the indicated error range	37	32	38	36
Number of γ-lines, whose uncertainties fall in the indicated error range	76	98	124	181

A comparison of Tables 5 and 6 shows the progress made by the measurement of k_0-factors and their introduction into "standard free" activation analysis: The number of reactions whose best γ-lines have an error <2% is 69; out of the k_0-values of these reactions 101 have errors <2%.

A list of k_i-**values** used in our laboratory is given in Table 7. The errors of the k_i-values are the standard deviations of the weighted means

$$s_{k,i} = \frac{\sqrt{\sum_j k_{i,j}^2 w_j}}{\sum_j w_j} \qquad (38)$$

where $k_{i,j} = C_{Au} h_j / k_{0,j}^{Au}$ and the symbols are the same as with Equations (24) and (25).

The percentage errors as indicated in Table 7 are

Element	Nuclide	Half-life	($f_{t1/2}$ %)	k_i	(f_{ki} %)	Δk_i(%)	Q_0	(f_{Q0} %)	$\bar{E}_r$	($f_{\bar{E}r}$ %)
Sodium	^{24}Na	14.659 h	(0.03)	74.393	(0.5)	0.0	0.59	(?)	3380.0	(11.0)
Magnesium	^{27}Mg	9.642 min	(0.12)	9854.1	(0.7)	0.0	0.64	(?)	2.57×10^5	(13.0)
Aluminium	^{28}Al	2.2407 min	(0.02)	198.25	(0.8)	0.0	0.71	(?)	11800.0	(5.9)
Silicon	^{31}Si	2.622 h	(0.02)	16749.0 [1]	(0.7)	15.5	5.83	(?)	2280.0	(0.4)
Sulfur	^{37}S	5.05 min	(0.40)	1.6656×10^6	(1.8)	0.1	1.12	(?)	-	(-)
Chlorine	^{38}Cl	37.24 min	(0.13)	573.33	(1.4)	-0.2	0.69	(?)	13700.0	(14.0)
Potassium	^{42}K	12.36 h	(0.02)	664.35	(2.5)	-0.1	0.97	(?)	2960.0	(7.1)
Calcium	^{47}Ca	4.536 d	(0.04)	2.6522×10^6	(2.2)	-1.2	1.3	(?)	-	(-)
Calcium	^{47}Sc	3.341 d	(0.09)	2.7528×10^6	(1.6)	2.5	1.3	(?)	-	(-)
Calcium	^{49}Ca	8.716 min	(0.13)	31636.0	(0.9)	-0.4	0.45	(?)	1.33×10^6	(-)
Scandium	^{46}Sc	83.83 d	(0.02)	2.8433	(0.4)	0.2	0.43	(?)	5130.0	(17.0)
Titanium	^{51}Ti	5.76 min	(0.17)	8629.1	(1.0)	0.2	0.67	(?)	63200.0	(4.0)
Vanadium	^{52}V	3.75 min	(0.27)	17.701	(1.2)	0.0	0.55	(?)	7230.0	(4.0)
Chromium	^{51}Cr	27.704 d	(0.01)	130.43	(0.5)	-0.2	0.53	(?)	7530.0	(11.0)
Manganese	^{56}Mn	2.5785 h	(0.02)	6.9201	(0.6)	0.9	1.053	(2.6)	468.0	(11.0)
Iron	^{59}Fe	44.497 d	(0.02)	25546.0	(1.1)	1.0	0.975	(1.0)	637.0	(24.0)
Cobalt	^{60}Co	5.2711 y	(0.02)	2.6262	(0.3)	-0.3	1.993	(2.7)	136.0	(5.1)
Nickel	^{65}Ni	2.52 h	(0.08)	6376.9	(2.3)	0.6	0.67	(?)	14200.0	(12.0)
Copper	^{64}Cu	12.701 h	(0.02)	33.681 [1]	(4.4)	-5.8	1.14	(?)	1040.0	(4.8)
Copper	^{66}Cu	5.1 min	(0.39)	138.03	(0.5)	0.0	1.06	(?)	766.0	(17.0)
Zinc	^{65}Zn	244.1 d	(0.09)	307.51	(0.4)	-0.1	1.908	(4.9)	2560.0	(10.0)
Zinc	^{69m}Zn	13.76 h	(0.15)	8263.7	(0.6)	0.0	3.19	(1.4)	590.0	(10.0)
Gallium	^{72}Ga	14.1 h	(0.14)	63.053 [1]	(0.5)	0.2	6.63	(5.2)	154.0	(12.0)
Germanium	^{75m}Ge	47.7 s	(1.5)	2332.2 [1]	(10.0)	16.8	2.41	(?)	3540.0	(7.9)
Germanium	^{75}Ge	1.3797 h	(0.05)	706.66 [1]	(7.1)	8.5	1.96	(?)	3540.0	(7.9)
Germanium	^{77m}Ge	52.9 s	(1.13)	3388.0 [1]	(10.0)	3.7	12.0	(?)	583.0	(4.0)
Germanium	^{77}Ge	11.3 h	(0.09)	23082.0 [1]	(3.4)	-9.8	13.3	(?)	583.0	(4.0)
Arsenic	^{76}As	26.328 h	(0.27)	32.151	(2.4)	-0.2	13.6	(?)	106.0	(34.0)
Selenium	^{75}Se	119.77 d	(0.01)	293.20 [1]	(1.1)	3.0	10.0	(?)	29.4	(4.1)
Bromine	^{80}Br	4.42 h	(0.23)	32.727	(10.2)	-2.4	11.0	(?)	69.3	(9.0)

[1] Calculated from k_0-values of Ref.[23].

(Table continued on next page)

Table 7 - k_0- values and other nuclear data (continued)

Element	Nuclide	Half-life	($f_{t1/2}$ %)	k_i	(f_{ki} %)	Δk_i(%)	Q_0	(f_{Q0} %)	$\bar{E}_r$	($f_{\bar{E}r}$ %)
Bromine	^{82}Br	1.4708 d	(0.05)	104.38	(0.5)	0.1	19.3	(5.1)	152.0	(9.2)
Rubidium	^{86}Rb	18.66 d	(0.11)	398.18	(1.0)	0.0	14.8	(2.5)	839.0	(4.0)
Rubidium	^{88}Rb	17.8 min	(0.56)	4981.4	(2.8)	-0.3	23.3	(2.9)	364.0	(3.0)
Strontium	^{85m}Sr	1.1258 h	(0.11)	42475.0	(10.0)	-0.3	14.5	(2.3)	469.0	(7.0)
Strontium	^{85}Sr	64.84 d	(0.03)	32859.0	(0.9)	0.0	13.25	(?)	469.0	(7.0)
Strontium	^{87m}Sr	2.795 h	(0.47)	1916.3	(0.5)	0.0	4.11	(1.7)	795.0	(2.0)
Yttrium	^{90m}Y	3.19 h	(0.31)	1.4164×10^5	(0.9)	-0.2	5.93	(2.3)	4300.0	(8.0)
Zirconium	^{95}Zr	64.02 d	(0.06)	16403.0	(0.4)	-0.2	5.05	(2.0)	6260.0	(4.0)
Zirconium	^{95}Nb	34.97 d	(0.09)	15251.0	(0.9)	-7.8	5.05	(2.0)	6260.0	(4.0)
Zirconium	^{97}Zr	16.9 h	(0.30)	2.5126×10^5	(6.1) [2]	-1.1	248.0	(1.5)	338.0	(2.1)
Zirconium	^{97m}Nb	60.0 s	(13.0)	2.6208×10^5	(0.9)	3.1	248.0	(1.5)	338.0	(2.1)
Zirconium	^{97}Nb	1.202 h	(1.00)	2.6180×10^5	(0.9)	3.0	248.0	(1.5)	338.0	(2.1)
Niobium	^{94m}Nb	6.26 min	(0.16)	178.83	(1.6)	0.0	7.35	(2.7)	574.0	(8.0)
Molybdenum	^{99}Mo	2.7477 d	(0.01)	4996.7	(1.4)	-0.9	53.1	(6.3)	241.0	(20.0)
Molybdenum	^{99m}Tc	6.0661 h	(0.03)	5017.3	(0.5)	11.5	53.1	(6.3)	241.0	(20.0)
Molybdenum	^{101}Mo	14.6 min	(0.68)	8642.5	(1.8)	4.3	18.84	(4.3)	672.0	(14.0)
Molybdenum	^{101}Tc	14.2 min	(0.70)	8231.4	(5.9)	-0.5	18.84	(4.3)	672.0	(14.0)
Ruthenium	^{97}Ru	2.88 d	(1.40)	13291.0	(0.5)	0.1	26.5	(3.5)	776.0	(16.0)
Ruthenium	^{103}Ru	39.245 d	(0.02)	459.83	(2.2)	0.4	3.63	(?)	181.0	(3.9)
Ruthenium	^{105}Ru	4.44 h	(0.45)	1804.3	(1.5)	-1.3	12.8	(2.7)	495.0	(10.1)
Ruthenium	^{105m}Rh	45.0 s	(?)	1885.5	(1.3)	0.8	12.8	(2.7)	495.0	(10.1)
Ruthenium	^{105}Rh	1.4733 d	(0.17)	1844.6	(2.7)	-3.5	12.8	(2.7)	495.0	(10.1)
Rhodium	^{104}Rh	4.34 min	(1.15)	1.1342	(10.0)	-12.3	7.5	(?)	1.45	(0.7)
Palladium	^{109}Pd	13.7 h	(0.73)	74.288 [1]	(2.6)	-2.5	28.8	(?)	39.7	(5.0)
Palladium	^{109m}Ag	39.6 s	(0.51)	73.039 [1]	(10.0)	-4.3	28.8	(?)	39.7	(5.0)
Palladium	^{111m}Pd	5.5 h	(1.81)	1.0894×10^5 [1]	(1.4)	-15.3	20.0	(?)	950.0	(9.
Silver	^{108}Ag	2.37 min	(0.42)	10.316	(4.6)	-1.2	2.9	(?)	38.5	(4.9)
Silver	^{110m}Ag	249.76 d	(0.02)	93.004 [1]	(0.6)	-2.5	17.5	(?)	6.08	(1.0)
Cadmium	^{111m}Cd	48.6 min	(0.62)	43080.0	(10.0)	0.1	112.0	(?)	125.0	(12.8)
Cadmium	^{115}Cd	2.228 d	(0.18)	2789.7	(10.0)	-5.9	39.6	(1.3)	207.0	(19.0)

[1] Calculated from k_0-values of Ref.[23].

[2] This error seems rather high for a flux monitor nuclide. Indeed, not ^{97}Zr but the 743 keV line of its daughter ^{97m}Nb is used and the smaller error with this nuclide is valid for this application.

(Text continued on next page)

Table 7 - k_i- values and other nuclear data (continued)

Element	Nuclide	Half-life	($f_{t1/2}$ %)	k_i	(f_{ki} %)	Δk_i(%)	Q_0	(f_{Q0} %)	$\bar{E}_r$	($f_{\bar{E}r}$ %)
Cadmium	^{115m}In	4.4861 h	(0.09)	2852.7	(10.0)	-3.5	39.6	(1.3)	207.0	(19.0)
Indium	^{114m}In	49.51 d	(0.02)	508.08 [1]	(2.3)	-6.4	27.3	(?)	6.41	(15.0)
Indium	^{116m}In	54.15 min	(0.01)	1.2435	(1.2)	-2.0	16.8	(1.9)	1.56	(1.9)
Tin	^{113}Sn	115.09 d	(0.03)	32381.0 [1]	(1.2)	-16.0	48.4	(1.2)	107.0	(2.8)
Tin	^{113m}In	1.658 h	(0.06)	37184.0 [1]	(0.8)	-1.0	48.4	(1.2)	107.0	(2.8)
Tin	^{117m}Sn	13.61 d	(0.29)	2.2579×10^5 [1]	(1.0)	-0.8	56.3	(1.9)	128.0	(3.
Tin	^{123m}Sn	40.08 min	(0.17)	29115.0 [1]	(0.5)	-0.1	5.4	(0.7)	424.0	(14.0)
Tin	^{125m}Sn	9.52 min	(0.53)	29275.0 [1]	(2.0)	-0.2	60.1	(2.9)	74.2	(7.0)
Tin	^{125}Sn	9.64 d	(0.43)	7.0289×10^5 [1]	(15.4)	-15.3	60.1	(?)	74.2	(7.0
Tin	^{125}Sb	2.73 y	(1.10)	8.6652×10^5 [1]	(4.1)	6.5	60.1	(?)	74.2	(7.0
Antimony	^{122}Sb	2.7 d	(0.37)	55.736	(1.5)	0.0	33.0	(3.5)	13.1	(3.8)
Antimony	^{124}Sb	60.2 d	(0.05)	116.00	(0.4)	0.0	28.8	(3.7)	28.2	(6.4)
Tellurium	^{131}I	8.04 d	(0.01)	3221.7 [1]	(1.6)	2.9	2.5	(?)	2950.0	(7.1)
Iodine	^{128}I	24.99 min	(0.08)	51.977 [1]	(7.5)	-0.3	24.8	(2.7)	57.6	(4.0)
Cesium	^{134m}Cs	2.91 h	(0.35)	80.403	(1.7)	-0.2	11.8	(3.0)	9.27	(11.0)
Cesium	^{134}Cs	2.062 y	(0.25)	7.1838	(0.8)	-0.1	12.7	(?)	9.27	(11.0)
Barium	^{131m}Ba	14.65 s	(1.3)	2.3052×10^5	(10.0)	4.8	23.5	(?)	69.9	(5.0)
Barium	^{131}Ba	11.8 d	(1.70)	23675.0	(1.2)	-0.5	24.8	(?)	69.9	(5.0)
Barium	^{133m}Ba	1.6209 d	(0.25)	2.7510×10^5	(10.0)	-0.1	5.6	(?)	143.0	(-)
Barium	^{139}Ba	1.41 h	(0.5)	785.07	(0.7)	0.0	0.88	(?)	15700.0	(3.2)
Lanthanum	^{140}La	1.678 d	(0.02)	24.724	(0.8)	0.0	1.24	(?)	76.0	(3.9)
Cerium	^{141}Ce	32.5 d	(0.03)	456.89	(0.9)	-0.1	0.83	(?)	7200.0	(18.0)
Cerium	^{143}Ce	1.375 d	(0.60)	2144.8	(0.7)	-0.4	1.2	(?)	1540.0	(120)
Praseodymium	^{142}Pr	19.13 h	(0.21)	20.975	(0.6)	0.4	1.51	(?)	296.0	(4.1)
Neodymium	^{147}Nd	10.98 d	(0.09)	964.99	(1.6)	0.4	2.0	(1.2)	874.0	(5.9)
Neodymium	^{149}Nd	1.73 h	(0.58)	1689.0	(3.1)	-4.3	5.08	(2.5)	236.0	(5.9)
Neodymium	^{149}Pm	2.2117 d	(0.09)	1763.1	(1.1)	0.1	5.08	(2.5)	236.0	(5.9)
Neodymium	^{151}Nd	12.44 min	(0.56)	4499.5	(7.4)	-3.7	12.3	(0.8)	173.0	(12.0)
Neodymium	^{151}Pm	1.1833 d	(0.14)	4592.4	(10.0)	-1.6	12.3	(0.8)	173.0	(12.0)
Samarium	^{153}Sm	1.9459 d	(0.20)	4.2506	(2.1)	0.0	14.4	(2.1)	8.53	(1.1)

[1] Calculated from k_0-values of Ref.[23].

(Table continued on next page)

Table 7 - k_I- values and other nuclear data (continued)

Element	Nuclide	Half-life	($f_{t1/2}$ %)	k_i	(f_{ki} %)	Δk_i(%)	Q_0	(f_{Q0} %)	$\bar{E}_r$	($f_{\bar{E}r}$ %)
Samarium	^{155}Sm	22.1 min	(0.90)	142.61	(4.1)	0.4	4.3	(7.0)	142.0	(7.0)
Europium	^{152m}Eu	9.32 h	(0.11)	0.16840 [1]	(8.7)	10.2	0.44	(?)	-	(-)
Europium	^{152}Eu	13.33 y	(0.30)	0.07753 [1]	(0.3)	-6.5	0.67	(?)	-	(-)
Europium	^{154}Eu	8.8003 y	(1.14)	1.5732	(0.9)	-0.1	5.66	(?)	5.8	(4.0)
Gadolinium	^{153}Gd	241.6 d	(0.08)	164.34 [1]	(8.1)	-8.1	2.75	(?)	-	(-)
Gadolinium	^{159}Gd	18.56 h	(0.43)	440.82 [1]	(19.3)	0.6	31.0	(4.5)	48.2	(8.0)
Gadolinium	^{161}Gd	3.7 min	(2.7)	743.86	(4.6)	-6.3	3.83	(1.9)	480.0	(7.1)
Terbium	^{160}Tb	72.3 d	(0.28)	11.080	(0.4)	-0.1	17.9	(3.8)	18.1	(5.0)
Dysprosium	^{165m}Dy	75.48 s	(0.48)	0.56253	(7.6)	-0.2	0.25	(?)	224.0	(4.9)
Dysprosium	^{165}Dy	2.334 h	(0.26)	0.35109	(5.6)	0.0	0.19	(19.3)	224.0	(4.9)
Holmium	^{166}Ho	26.808 h	(1.10)	4.5305 [1]	(2.8)	-4.0	10.95	(2.5)	12.3	(3.3)
Erbium	^{171}Er	7.52 h	(0.40)	214.73 [1]	(1.4)	1.9	4.42	(3.3)	129.0	(2.3)
Thulium	^{170}Tm	128.6 d	(0.23)	3.4694 [1]	(1.7)	24.4	14.5	(?)	4.8	(2.1)
Ytterbium	^{169}Yb	32.022 d	(0.03)	78.338 [1]	(4.4)	-4.5	6.4	(?)	0.61	(1.6)
Ytterbium	^{175}Yb	4.19 d	(0.24)	7.0173	(6.4)	-0.6	0.46	(?)	602.0	(8.0)
Ytterbium	^{177}Yb	1.9 h	(5.3)	725.02	(6.9)	-0.3	2.5	(1.8)	412.0	(5.1)
Ytterbium	^{177}Lu	6.71 d	(0.15)	744.62	(10.0)	2.3	2.5	(1.8)	412.0	(5.1)
Lutetium	^{176m}Lu	3.635 h	(0.08)	17.848	(1.5)	-0.1	34.8	(3.1)	16.1	(5.0)
Lutetium	^{177}Lu	6.71 d	(0.15)	5.3426 [1]	(5.1)	-0.5	0.52	(?)	-	(-)
Hafnium	^{175}Hf	70.0 d	(2.85)	333.15	(1.0)	0.0	0.78	(?)	29.6	(7.1)
Hafnium	^{180m}Hf	5.5189 h	(0.07)	4811.8	(1.5)	-0.4	14.4	(2.4)	16.2	(11.7)
Hafnium	^{181}Hf	42.39 d	(0.14)	62.460	(1.2)	-0.1	2.52	(3.6)	115.0	(6.1)
Tantalum	^{182}Ta	115.0 d	(0.17)	14.795 [1]	(1.0)	0.4	33.3	(?)	10.4	(5.8)
Tungsten	^{187}W	23.9 h	(0.42)	27.517	(1.8)	-0.2	13.7	(1.8)	20.5	(1.0)
Rhenium	^{186}Re	3.777 d	(0.11)	7.7784	(14.4)	-0.3	15.4	(2.5)	3.4	(4.1)
Rhenium	^{188m}Re	18.6 min	(0.54)	239.36	(3.7)	-0.7	4.57	(6.4)	41.1	(3.9)
Rhenium	^{188}Re	16.98 h	(0.12)	6.7032	(3.3)	-0.7	4.34	(6.4)	41.1	(3.9)
Osmium	^{185}Os	93.6 d	(0.53)	437.04	(1.5)	0.0	0.43	(?)	-	(-)
Osmium	^{191}Os	15.4 d	(0.65)	308.78	(1.6)	0.7	2.03	(?)	114.0	(1.8)
Osmium	^{193}Os	1.2709 d	(1.35)	251.86	(2.4)	2.0	2.34	(?)	89.7	(4.0)

[1] Calculated from k_0-values of Ref.[23].

(Table continued on next page)

Element	Nuclide	Half-life	($f_{t1/2}$ %)	k_i	(f_{ki} %)	Δk_i(%)	Q_0	(f_{Q0} %)	$\bar{E}_r$	($f_{\bar{E}r}$ %)
Iridium	^{192}Ir	73.831 d	(0.01)	0.93030 [2]	(4.7)	-	5.8	(?)	-	(-)
Iridium	^{194}Ir	19.15 h	(0.16)	4.3925	(7.6)	-0.8	12.0	(2.9)	2.21	(9.0)
Platinum	^{191}Pt	2.9 d	(3.50)	16783.0 [2]	(10.0)	-	0.44	(?)	27.6	(2.2)
Platinum	^{195m}Pt	4.02 d	(0.25)	27312.0 [2]	(10.0)	-	142.5	(?)	-	(-)
Platinum	^{197}Pt	18.3 h	(1.70)	3231.3 [2]	(10.0)	-	14.0	(?)	291.0	(15.1)
Platinum	^{199}Pt	30.8 min	(1.30)	1420.4 [2]	(10.0)	-	17.0	(1.8)	106.0	(2.8)
Platinum	^{199}Au	3.139 d	(0.22)	1253.5	(2.7)	-0.3	17.0	(1.8)	106.0	(2.8)
Gold	^{198}Au	2.6935 d	(0.01)	3.3153	(0.0)	0.0	15.71	(1.8)	5.65	(7.1)
Mercury	^{197m}Hg	23.8 h	(0.42)	2363.9	(1.0)	0.4	0.49	(?)	93.5	(0.1)
Mercury	^{197}Hg	2.6725 d	(0.08)	69.889 [2]	(6.3)	-	0.4	(?)	93.5	(0.1)
Mercury	^{203}Hg	46.6 d	(0.04)	256.92	(1.7)	0.0	0.88	(?)	1960.0	(8.2)
Thorium	^{233}Pa	27.0 d	(0.37)	53.178	(1.0)	0.2	11.53	(3.6)	54.4	(0.9)
Uranium	^{239}U	3.47 min	(0.21)	136.17 [1]	(1.2)	-6.3	103.4	(1.3)	16.9	(1.2)
Uranium	^{239}Np	2.355 d	(0.17)	139.03 [1]	(2.1)	-4.1	103.4	(1.3)	16.9	(1.2)
Uranium	^{95}Zr	64.02 d	(0.06)	1438.7 [3]	(7.1)	-	0.47	(?)	-	(-)
Uranium	^{103}Ru	39.245 d	(0.02)	3140.5 [3]	(7.4)	-	0.47	(?)	-	(-)
Uranium	^{131}I	8.04 d	(0.01)	3255.3 [3]	(5.8)	-	0.47	(?)	-	(-)
Uranium	^{137}Cs	30.001 y	(0.67)	1520.8 [3]	(10.0)	-	0.47	(?)	-	(-)
Uranium	^{140}Ba	12.747 d	(0.08)	1516.6 [3]	(5.0)	-	0.47	(?)	-	(-)
Uranium	^{140}La	1.678 d	(0.02)	1517.2 [3]	(4.1)	-	0.47	(?)	-	(-)
Uranium	^{141}Ce	32.5 d	(0.03)	1666.7 [3]	(10.0)	-	0.47	(?)	-	(-)
Uranium	^{147}Nd	10.98 d	(0.09)	4147.1 [3]	(5.0)	-	0.47	(?)	-	(-)
Uranium	^{155}Eu	4.9602 y	(0.20)	2.9410×10^5 [3]	(7.1)	-	0.47	(?)	-	(-)

[1] Calculated from k_0-values of Ref.[23].

[2] Calculated from basic nuclear data by Equation (26).

[3] Calculated from basic nuclear data by Equation (26), where instead of $\sigma_{th,x}$ the value of $\sigma_{f,U\text{-}235} \times y_{f,U\text{-}235}$ is inserted. $\sigma_{f,U\text{-}235}$, the fission cross-section, is 583.5 b. $y_{f,U\text{-}235}$ are the cumulative fission yields [25], which are mostly identical with the chain yields, because the nuclides considered are usually at or near to the end of the decay chaines.

$$f_{k,i} = \frac{s_{k,i}}{k_i} \times 100 \qquad (39)$$

With k_i-values calculated from nuclear constants errors were set to 10%. With k_i-values calculated from not recommended k_0-values errors of k_i were calculated by the above equations; the errors of k_0 were set to 10%.

The differences between the k_0-based and the "theoretical" k_i-values calculated by Equation (26) are shown under Δk_i. With some exceptions they are <2% and confirm both the accuracies of the k_0- and of the k_i-values. With those nuclides where Δk_i >2% it is still necessary, to check and to re-measure the values of the nuclear constants, mainly the γ-ray- and the isotopic abundances. In many cases the discrepancies concern reactions with branched activation and decay and here the branching ratios may be unclear. The errors of k_i-factors are often smaller than those of the k_0-values because they are mean values. This does not mean, that the k_i-method is more accurate, because also with the k_0-method mean values will be calculated if more than one γ-peak is used for the evaluation.

The traceability of the k_i-values is comparable to that of the k_0-values, but additional reference has to be made to the sources of the γ-ray abundances. Since the publication of our γ-ray tables [6] some new compilations have been published out of which the French "Table de Radionucléides" [14], which contains only selected radionuclides, and the "Table of the Radioactive Isotopes" [13] have to be mentioned.

Errors of Q_0-***values*** have a low propagation factor on the analytical results, because they act only by Φ_{epi}/Φ_{th}, the reciprocal flux ratio, which is with most reactor irradiation facilities between 1/20 and 1/500. Out of the ≃100 Q_0-values listed in Ref. [10] two thirds have errors below 10%, but with one third no errors are indicated (see Table 7), because they are, until now, measured by only one laboratory and discrepancies to other values found in compilations are too large. Although we can assume, that their uncertainties are also within ±10%, re-measurements and appropriate indications of their errors are desirable to have a complete data set for the estimation of analytical errors and to fill this gap in the traceability. This holds especially for those elements having high Q_0-values (which include such important nuclides as ^{76}As, ^{75}Se, ^{85}Sr, ^{110m}Ag, ^{114m}In, ^{134}Cs, ^{170}Tm, and ^{182}Ta).

The errors of the ***effective resonance energies,*** $\bar{E}_r$, have even less influence on the analytical results than those of the Q_0-values. As has been outlined by JOVANOVIC et al.[24], uncertainties in $\bar{E}_r$ of ≃50% will be tolerable even in the most unfavourite cases when reactions with high Q_0-values have to be used. Therefore, we can cope with the fact, that many $\bar{E}_r$-values have errors >10% and that, strictly speaking, $\bar{E}_r$-factors are not constants, i.e. their values depend on the shape of the epithermal neutron spectrum.

Decay constants or half-lives are accurately known with all nuclides important in activation analysis. From Table 7 we can see that with ≃50% of all nuclides the errors of $t_{1/2}$ are <0.2% and with only ≃10% they are >2%. The error propagation factor depends on the length of the irradiation, the waiting and the counting time according

to the time factor Z. As long as the ratio of one of these periods to the half-life is not larger than ≃10, the propagation factor is small.

4d. Errors with the parameters of the time dependent term and their propagation

The error propagation law for the time dependent term

$$s_Z^2 = \left(\frac{\partial Z}{\partial \lambda} s_\lambda\right)^2 + \left(\frac{\partial Z}{\partial t_i} s_{t,i}\right)^2 + \left(\frac{\partial Z}{\partial t_w} s_{t,w}\right)^2 + \left(\frac{\partial Z}{\partial t_m} s_{t,m}\right)^2 \qquad (40)$$

yields

$$\frac{s_Z^2}{Z^2} = \frac{s_\lambda^2}{\lambda^2} + s_\lambda^2 t_w^2 + s_{tw}^2 \lambda^2 + \frac{s_\lambda^2 t_i^2 + s_{ti}^2 \lambda^2}{e^{2\lambda t_i}\left(1 - e^{-\lambda t_i}\right)^2} + \frac{s_\lambda^2 t_m^2 + s_{tm}^2 \lambda^2}{e^{2\lambda t_m}\left(1 - e^{-\lambda t_m}\right)^2} \qquad (41)$$

i.e. the propagation of errors of t_i, t_w, t_m and especially of λ is rather complex. Estimations of errors are given in Table 8.

With the ***irradiation time*** we have to be aware of the fact that this parameter occurs in the Z-terms of Equation 27 for the calculation of the amounts of elements and in those of Equations 28 and 29 for the calculation of the fluxes and its value and error is identical, if monitors and samples are irradiated together, as it is usually done. Then, the propagation of errors is still more complicated than those of the errors with the other parameters of the Z-term. Some examples have been calculated and the results are shown in Figures 14 - 17.

As examples nuclides with short (^{51}V), medium (^{56}Mn, ^{24}Na, ^{76}As) and long (^{59}Fe, ^{60}Co) half-lives are chosen and short (Fig. 14), medium (Fig. 15 and 16) and long (Fig. 17) half-lives are considered. The error propagation factors were calculated assuming the following case: The true weight of the sample is m, and the true fluxes are Φ_{th} and Φ_{epi}. The irradiation time was chosen to be $t_i = t_{i,chosen}$ but it happened that it became $t_{i,real} = t_{i,chosen}(1 + f_{ti})$, without the experimenter getting aware of this fault. During this irradiation time, $t_{i,real}$, in the flux monitor zirconium the activities A_{Zr-95} and A_{Zr-97} were generated. Using these activities with Equations 28 and 29 and inserting $t_{i,chosen}$ in Z_{Zr-95} and Z_{Zr-97}, wrong flux values will be calculated. With these fluxes and $t_{i,chosen}$ inserted in Z_x of Equation 27, a wrong amount of element, m_f, is found. The error propagation factor is then $p = (m_f - m)/(m\, f_{ti})$. Fortunately, the uncertainty of the irradiation time is with most irradiation experiments very small, (<0.1%), so that its influence on the analytical results is negligible.

With the ***waiting time***, the propagation of errors depends on the ratio $t_w/t_{1/2}$ and on the size of the error itself, as is shown in Figure 18.

The influence of errors of the ***counting time***, t_m, is presented in Figure 19. These errors are mainly caused by the dead time of the counting equipment. Some experiences with the automatic dead time correction of a γ-ray spectrometer shall be reported.

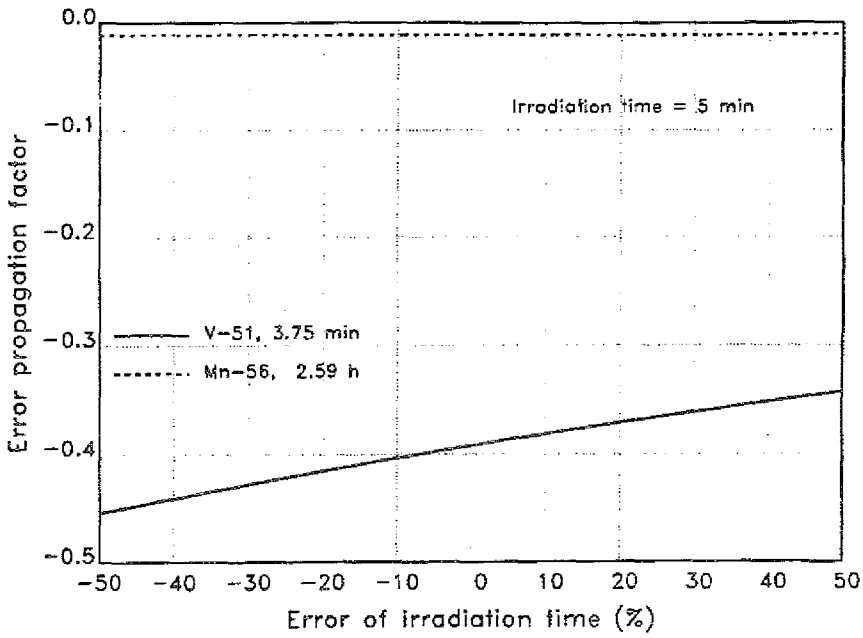

Figure 14 - Influence of errors of the irradiation time. Example: irradiation time 5 min, nuclides ^{51}V and *Mn* presup 56 .

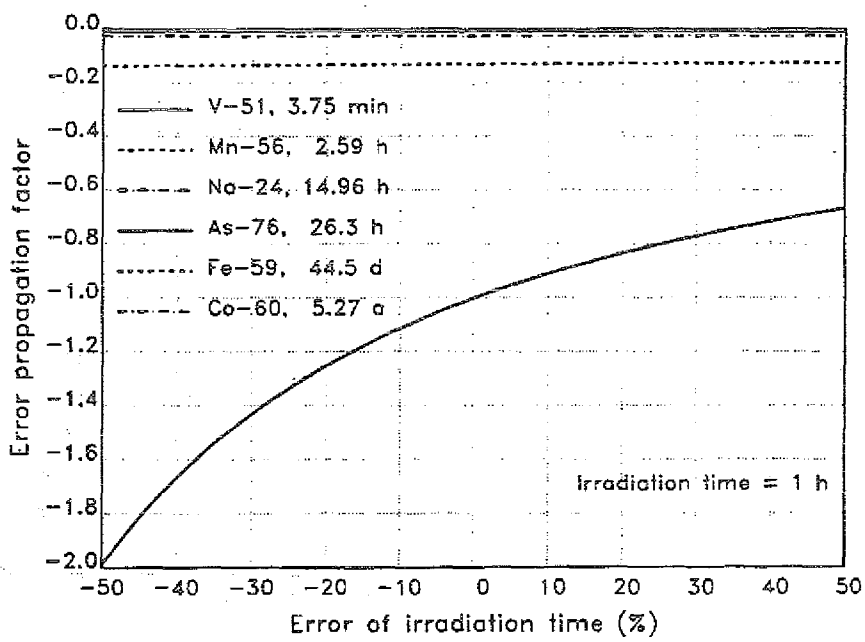

Figure 15 - Influence of errors of the irradiation time. Example: irradiation time 1 hour..

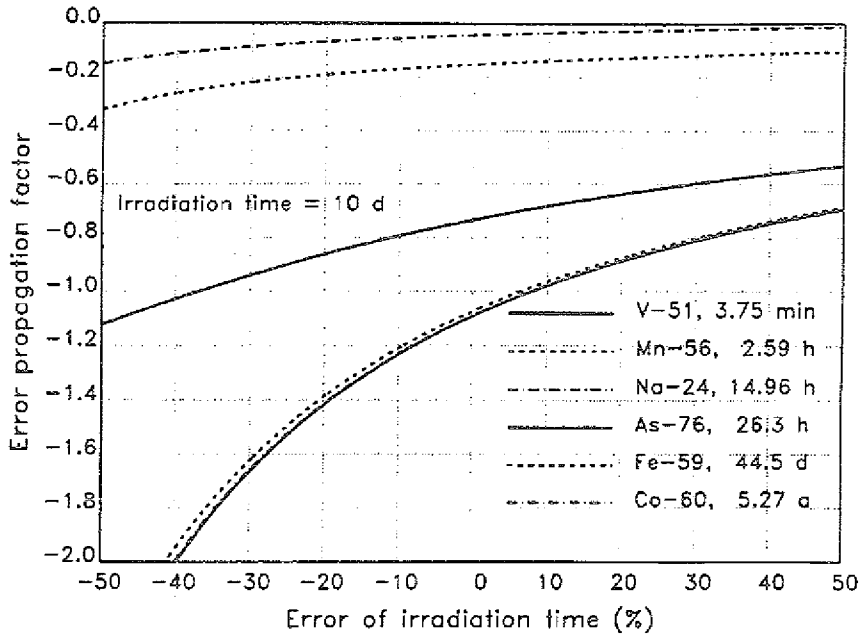

Figure 16 - Influence of errors of the irradiation time. Example: irradiation time 1 day.

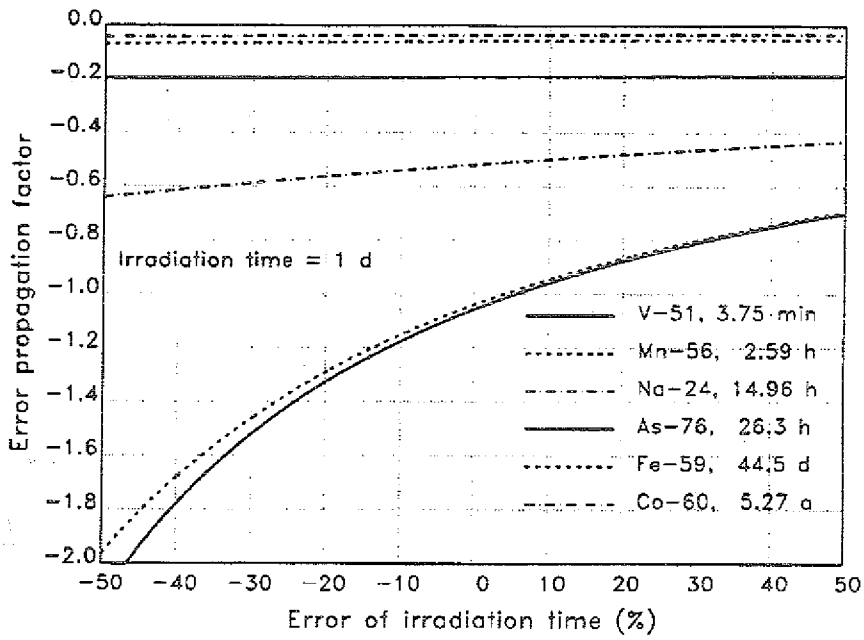

Figure 17 - Influence of errors of the irradiation time. Example: irradiation time 10 days.

Table 8 - Contributions to the error of the time dependent term, Z

• **Half-life, decay constant, $t_{1/2}, \lambda$** *With some nuclides the error is larger, see Tables 6 and 7.*	**<2%**
• **Irradiation time, t_i** *Is usually correct within ±1 s and with fast rabbit tube facilities much better. Uncontrollable errors may occur if the in- and output times are not correctly recorded. They are avoided with irradiation facilities where these events are recorded automatically. The influence of errors of t_i is rather complicated, because it acts, with different propagation factors, on the time dependent terms in the flux calculation (with ^{95}Zr and ^{97}Zr) and of the nuclide to be measured. Error propagation factors, depending on the size of the error of t_i, are shown for several irradiation times and nuclides in Fig. 14.*	**<0.1%**
• **Waiting time, t_w** *Here, similar considerations as with the irradiation time are valid, except those with the error propagation factors. They depend strongly on the ratio $t_w/t_{1/2}$ (see Fig. 15).*	**<0.1%**
• **Counting time, measuring time, t_m** *Although the clock time can exactly be measured, the dead time correction is not always accurate and depends on the equipment used. Details are described in the text.*	**1-5%**
Error of the time dependent term, Z *It is mainly determined by the error of the counting time. If the waiting time is very long and the error of the half-life is >2% higher errors may occur.*	**1-5%**

The dead time is caused by the time required for thetreatment of the signal generated in the detector until it is stored in the memory of the multichannel analyzer (MCA). To avoid pulse-pile-up effects, i.e. the summation of pulses reaching the detector within the resolution time of the pulse processing equipment (preamplifier, amplifier and analog-to-digital converter, ADC), no pulses are accepted during this time. Thus, the true counting time would be shortened by all the time periods when the equipment does not accept pulses, when it is "dead". Therefore, the dead time is added to the clock time to re-adjust the counting time chosen (automatic dead time correction). With "slow" ADC's the dead time is caused mainly by these units and automatic dead time corrections were carried out only with them. Meanwhile, very "fast" ADC's are available and the processing time in the amplifier is no longer negligible. With the systems in our laboratory, containing ADC's ND583 and amplifiers Silena S7611 or Canberra C2020, it was found that the automatic dead time correction was wrong by up to 40%. Only with low counting rates, generating a dead time of ≃5%, a reliable correction to ±0.5% was possible. After consulting the manufacturers, the amplifiers were modified and the automatic corrections became accurate to ≃±5%, when counting rates up to 40,000 counts per second were applied. Further improvement came with the introduction of the "pulser technique". Pulses were fed from a generator with stable pulse height and repetition rate to the

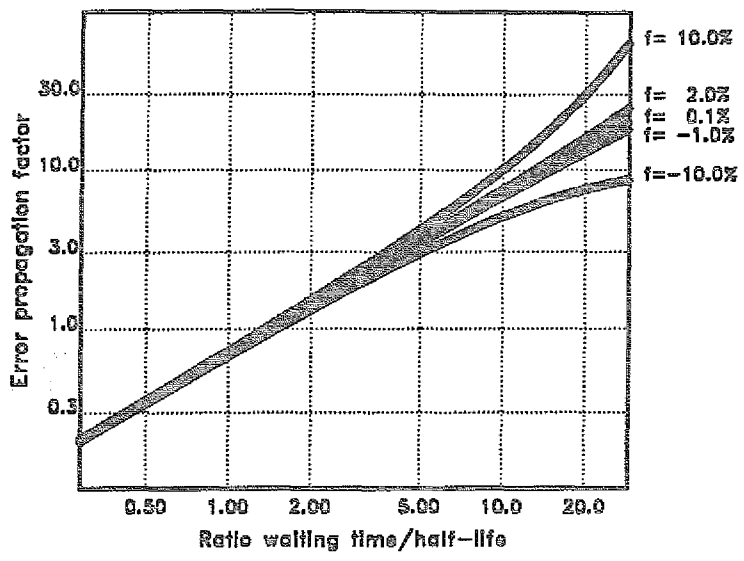

Figure 18 - Influence of errors of the waiting time.

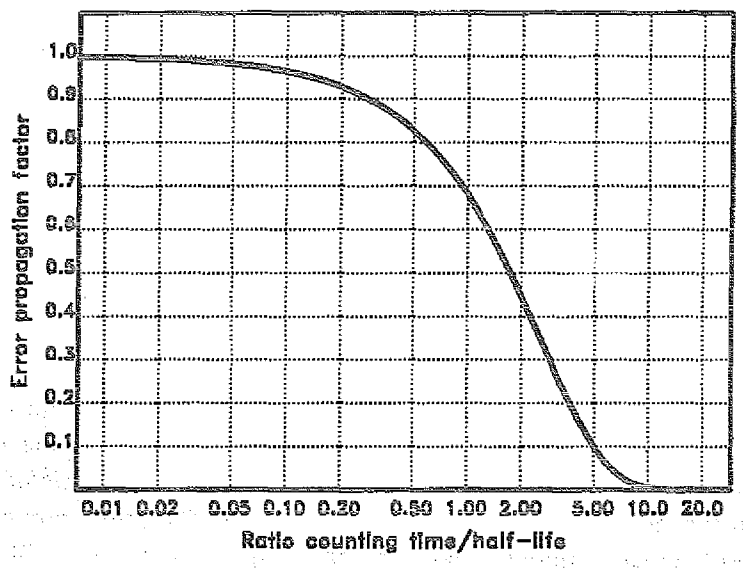

Figure 19 - Influence of errors of the counting time.

preamplifier and registered together with the pulses from the detector in the γ-spectrum. The chance of pulses to be rejected are the same for those of the detector and those of the generator. Thus from the number of pulses collected in the generator peak, the dead time can be calculated and corrected for. With this technique, errors were <1% with counting rates up to 40,000 counts per second. A similar improvement was attained with Westphals's Loss Free Counting module (ND599), which, however, also required modifications of amplifiers and the ADC's. After these experiments and experiences we estimate the error of the dead time to <1%, if counting rates are not too high (< 40,000 counts per

second) and the pulser technique or the ND599 is used. If the equipment is not carefully checked and optimized, dead time errors can be much larger. The propagation factor with the error of the counting time is $\simeq 1$, because usually $t_m \ll t_{1/2}$ (see Figure 19).

4e. Errors with the flux term

The flux term is $\Psi = \Phi_{th} + \Phi_{epi} Q_\alpha$ and the square of its relative error is

$$\frac{s_\Psi^2}{\Psi^2} = \frac{s_{\Phi th}^2 + s_{\Phi epi}^2 Q_\alpha^2 + s_{Q\alpha}^2 \Phi_{epi}^2}{(\Phi_{th} + \Phi_{epi} Q_\alpha)^2} \tag{42}$$

Here, Φ_{th}, Φ_{epi} and Q_α are again composed terms (Equations 28, 29 and 30). The square of the error of the cross section ratio is

$$s_{Q\alpha}^2 = \left(\frac{Q_0 - 0.429}{\bar{E}_r^\alpha} \right)^2 \left[\frac{s_{Q0}^2}{(Q_0 - 0.429)^2} + \left(\frac{s_{\bar{E}_r^\alpha}}{\bar{E}_r} \right)^2 + (s_\alpha \ln \alpha)^2 \right]$$
$$+ \left[\frac{0.429}{(2\alpha + 1)\, 0.55^\alpha} \right]^2 \left[\frac{4 s_\alpha^2}{(2\alpha + 1)^2} + (s_\alpha \ln \alpha)^2 \right] \tag{43}$$

The square of the error of the thermal flux is

$$s_{\Phi th}^2 = [m_{Zr}(Q_{\alpha,5} - Q_{\alpha,7})]^2$$
$$\times \left[(Q_{\alpha,5} A_7 k_{i,7} Z_7)^2 \left(\frac{s_{Q\alpha,5}^2}{Q_{\alpha,5}^2} + \frac{s_{A7}^2}{A_7^2} + \frac{s_{ki,7}^2}{k_{i,7}^2} + \frac{s_{Z7}^2}{Z_7^2} \right) \right.$$
$$+ (Q_{\alpha,7} A_5 k_{i,5} Z_5)^2 \left(\frac{s_{Q\alpha,7}^2}{Q_{\alpha,7}^2} + \frac{s_{A5}^2}{A_5^2} + \frac{s_{ki,5}^2}{k_{i,5}^2} + \frac{s_{Z5}^2}{Z_5^2} \right)$$
$$\left. + \frac{s_{m,Zr}^2}{m_{Zr}^2} + \frac{s_{Q\alpha,5}^2 + s_{Q\alpha,7}^2}{(Q_{\alpha,5} - Q_{\alpha,7})^2} \right] \tag{44}$$

and for that of the epithermal flux holds

Table 9 - How many reactions have errors >5% if utmost errors of α are estimated.

Irradiation facility	BE-4	BE-12	BE-20	FRM
Thermal neutron flux, Φ_{th}(n cm^{-2} s^{-1})	6.5×10^{12}	2.6×10^{13}	9.4×10^{13} 1.7×10^{13}	
Flux ratio, $R_\Phi = \Phi_{th}/\Phi_{epi}$	325	84	49	38
Epithermal flux shape factor, α	0.46	0.14	0.103	0.03
Largest error of α assumed	+70%	+40%	+30%	+30%
Number of reactions where results are wrong by >5%, if largest error comes true	12	3	1	0
Number of reactions where results are wrong by >5% if no α-correction is carried out	1	17	28	1

$$s^2_{\Phi epi} = [m_{Zr}(Q_{\alpha,5} - Q_{\alpha,7})]^2 \times \left[(A_7 k_{i,7} Z_7)^2 \left(\frac{s^2_{A5}}{A^2_5} + \frac{s^2_{ki,5}}{k^2_{i,5}} + \frac{s^2_{Z5}}{Z^2_5} \right) + (A_5 k_{i,5} Z_5)^2 \left(\frac{s^2_{A7}}{A^2_7} + \frac{s^2_{ki,7}}{k^2_{i,7}} + \frac{s^2_{Z7}}{Z^2_7} \right) + \frac{s^2_{m,Zr}}{m^2_{Zr}} + \frac{s^2_{Q\alpha,5} + s^2_{Q\alpha,7}}{(Q_{\alpha,5} - Q_{\alpha,7})^2} \right] \quad (45)$$

Although the uncertainties of some of the parameters of Equations 43 to 45 are large, the error of the flux term is usually small. The errors of Q_0 are often not known (see Table 7) and it has to be assumed, that they attain values of up to 10%. The errors of $\bar{E}_r$ are also listed in Table 7. The influence of the errors of Q_0 and $\bar{E}_r$ has been discussed in Section 3i.

The measurement of α-values can be difficult and errors of 10% - and, if the flux ratios Φ_{th}/Φ_{epi} are very high, even 40% - have to put up with. But their influence on the accuracies of analytical results is also small. A detailed documentation of the errors with

irradiation facilities used by the Radioanalytical Section of the ZCH is in preparation. [26] A summary of the results is given in Table 9. The reactions, for which errors of α have the largest influence on the results are ^{110m}Ag, ^{186}Re, ^{176m}Lu, ^{122}Sb, ^{182}Ta, ^{114m}In, ^{116m}In, and ^{239}Np.

5. Conclusion

As a conclusion with respect to the sources of error with absolute activation analysis using k_i-factors we have found, that all of the four terms of Equation 27 may usually have errors between 1 and 5%. They may be higher with samples not optimal for NAA.

With the activity term, A, the statistical counting error is often the predominant contribution, especially if low amounts of elements, near to the detection limit, have to be measured. Errors depending on the counting geometry can be reasonably corrected with samples not too large and of regular shape. But also with other types of samples these errors can be kept low and such sub-optimal samples have to be treated very often by NAA and it is one of its strong points, that this can be done.

With the Z-term the errors of irradiation and waiting times are usually negligible. Those of half-lives are sufficiently low, at least with the most important activation products and if waiting times do not exceed about five half-lives. The predominant component of the error is often the dead-time of the electronic equipment. The implementation of an accurate dead-time correction can become an expensive and time consuming enterprise.

With the flux term, the accuracies of the activities of the flux monitors and those of the k_0- or k_i-factors have the largest influence. Depending on the flux ratio, errors of Q_0 and α gain a predominant influence with some few nuclides having high Q_0-values. Another source of error is connected with the flux gradient in the irradiation facility. Since usually real samples have dimensions in the cm range (quartz or PE vials, solid pieces), its position within the irradiation facility should be well defined to ± 0.5 cm to keep the error $<0.2\%$.

With k_i-factors the errors are, at least with the important activation products, $<1\%$. It will be the determining component of the total error only, when nearly ideal samples have to be analyzed, so that geometrical counting errors and the flux gradient error is minimal, and when the activity is high enough to attain good counting statistics. In all other cases the uncertainties of k_i-factors (and the same holds for the other nuclear constants k_0, Q_0 and $\bar{E}_r$) are not the limiting factors of the accuracies of results of neutron activation analysis.

References

1 T. BRAUN *"Statistical Evaluation of Recorded Knowledge in Nuclear and Other Instrumental Techniques"* in IAEA-TECDOC-435, p.9 - 35. International Atomic Energy Agency, Wien 1987.

2 V.P.GUINN *"Activation Analysis in the Americas: Recent and Future Perspectives"*. 5th Int. Conf. Nucl. Meth. Environm. Energy Research, CONF-840408-DE84017348, p. 23 - 42 (1984)

3 G.J.LUTZ, R.J.BORENI, R.S.MADDOCK AND J.WING *"Activation Analysis: A Bibliography Through 1971"* NBS Technical Note 467, National Bureau of Standards, Washington, D.C. (1972)

4 W. SEELMANN-EGGEBERT, G. PFENNIG, H. MÜNZEL, W. KLEWE-NEBENIUS *"Karlsruher Nuklidkarte"*, 5. Aufl., Kernforschungszentrum Karlsruhe GmbH, 1981;
F. W. WALKER, J. R. PARRINGTON, F. FEINER *"Chart of the Nuclides"*, 14th edition; Knolls Atomic Power Laboratory, General Electric Company, San Jose, CA (1988).

5 G.ERDTMANN *"Neutron Activation Analysis with Research Reactors: Applications and Techniques"* in "Multipurpose Research Reactors", Proceedings of an International Symposium on the Utilization of Multipurpose Research Reactors and Related International Co-operation organized by the International Atomic Energy Agency and held in Grenoble, 19-23 October 1987, IAEA Wien 1988

6 G. ERDTMANN UND W. SOYKA *"The Gamma-Rays of the Radionuclides"* Verlag Chemie, Weinheim/Bergstraße, 1979.

7 C. H. WESTCOTT *"Effective cross section values for well-moderated thermal reactor spectra"* CRRP-960, Atomic Energy of Canada Ltd., 3rd ed. 1960

8 O.T.HØGDAHL *"Neutron Absorption in Pile Neutron Activation Analysis"*, MMPP-226-1, Dec. 1962.

9 F.GIRARDI, G.GUZZI, AND J.PAULY *Anal. Chem.* **37** 1085 (1965).

10 F.DECORTE, A.SIMONITS *J. Radioanal. Nucl. Chem.* **133**, 43 (1989).

11 A.SIMONITS, F.DECORTE, AND J.HOSTE *J. Radioanal. Chem.* **31**, 467 (1976).

12 R.GUNNINK AND J.B.NIDAY *"Computerized Quantitative Analysis by Gamma-Ray Spectrometry"* Report of the University of California Radiation Laboratory, UCRL-51061 , Vols. 1 - 3 (1972).

13 E. BROWNE AND R. B. FIRESTONE *"Table of Radioactive Isotopes"* John Wiley & Sons, New York, Chichester, Brisbane, Toronto, Singapore 1986

14 F.LAGOUTINE, N.COURSOL, AND J.LEGRAND *Table de Radionucléides* (new edition since 1982) Commissariat à l'Energie Atomique, Laboratoire de Métrologie des Rayonnements Ionisants, 91190 Gif-sur-Yvette , France.

15 F.DECORTE *"The k_0-Standardization Method. A Move to the Optimization of Neutron Activation Analysis"*. Thesis. Rijksuniversiteit Gent(Belgium), 1987.

16 W. HÄFELE *Bericht des Kernforschungszentrums Karlsruhe* **KFK-102**, 1962

17 F.DECORTE, L.MOENS, S.JOVANOVIC, A.SIMONITS, A.DEWISPELAERE *J. Radioanal. Nucl. Chem.* **102**, 37 (1986).

18 S.JOVANOVIC, F.DECORTE, A.SIMONITS, L.MOENS, P.VUKOTIC, J.HOSTE *J. Radioanal. Nucl. Chem.* **113** 177 (1987).

19 T. EL NIMR, F. DE CORTE, L. MOENS, A. SIMONITS, J. HOSTE *J. Radioanal. Chem.* **67** 421 (1981).

20 A.A.SMALES *"The place of activation analysis in geochemistry and cosmochemistry"*, in A. O. Brunfelt and E. Steinnes (Eds.) *"Activation Analysis in Geochemistry and Cosmochemistry"*, Universitetsforlaget Oslo - Bergen - Tromsö 1971

21 B.A.MARKERT *"Instrumentelle Multielementanalysen an Pflanzen"* VCH Verlag, Weinheim/Bergstraße, to be published 1991

22 G.ERDTMANN AND H.PETRI *"Nuclear Activation Analysis: Fundamentals and Techniques"* in Kolthoff-Elving *"Treatise on Analytical Chemistry"* (2nd Ed. by P.J.Elving), Part I, Vol. 14, p.419 ff. John Wiley & Sons, New York, (1986).

23 F.DECORTE, A.SIMONITS, F.BELLEMANS, M.C.FREITAS, S.JOVANOVIC, B.SMODIS, G.ERDTMANN, H.PETRI, A.DEWISPELAERE Paper presented at the 8th Conference *Modern Trends in Activation Analysis"*, Wien 1991., in print in *J. Radioanal. Nucl. Chem.* (1992).

24 S.JOVANOVIC, F.DECORTE, L.MOENS, A.SIMONITS, J.HOSTE *J. Radioanal. Nucl. Chem.* **82** 379 (1984).

25 E.A.C.Crouch *"Assessment of known independent yields and the calculation of those unknown in the fission of* ^{232}Th, ^{233}U, ^{235}U, ^{238}U, ^{239}Pu, ^{240}Pu *and* ^{241}Pu*". Report of the Atomic Energy Research Establishment Harwell,* **AERE - R 7680** , May 1974. Revised data of 1976/77, (private communication).

26 G.ERDTMANN *"Errors of Absolute Methods of Reactor Neutron Activation Analysis Caused by Non-1/E Epithermal Neutron Spectra. I. The Influence of the Error of* α *when Using the Zirconium Double-Monitor Method."* Report of the Research Center Jülich **JÜL-2670** (August 1992), in print.

FORSCHUNGSZENTRUM JÜLICH GmbH

KFA

Jül-2673
September 1992
ISSN 0366-0885